

1 Fugitive natural gas emissions in York, United Kingdom: Updating
2 the parameters of existing algorithms to be based on instrumental
3 limitations.~~Fugitive emissions of natural gas in York, United~~
4 ~~Kingdom: Adapting existing algorithms parameters to be based on~~
5 ~~instrument specifications.~~

6 Thomas C. Moore¹, James R. Hopkins^{1,2}, Will S. Drysdale^{1,2}, Stuart Young¹, Sri Hapsari Budisulistiorini¹,
7 Marvin D. Shaw^{1,2}, Mackenzie LeVernois³, James L. France^{3,4}, David Lowry³ and James D. Lee^{1,2}

8 ¹Wolfson Atmospheric Chemistry Laboratories, University of York, York YO10 5DD, United Kingdom

9 ²National Centre for Atmospheric Science, University of York, York YO10 5DD, United Kingdom

10 ³Royal Holloway, University of London, Earth Sciences, Egham, United Kingdom

11 ⁴Environmental Defence Fund Europe, Avenue des Arts 47-49, Brussels, Belgium

12
13
14 *Correspondence to:* james.lee@york.ac.uk
15

16 **Abstract**

17 Reducing methane emissions has become increasingly important in recent years due to its importance for radiative forcing.
18 One area of particular interest is the oil and gas sector, which often results in fugitive emissions of methane from natural gas
19 distribution. Of the many sources of methane, fugitive emissions from a country's domestic natural gas network are one that
20 can have a direct impact on the citizens of a country. Previous studies have shown the ability to detect these emissions by use
21 of mobile surveys measuring methane, some of these use secondary co-emitted compounds as a means of confirming the nature
22 of the emission. This study aims to adapt existing algorithms parameters by investigating the limitations of equipment used
23 within the platform used for mobile surveys. ~~This has led to reduced enhancement parameters as well as reduced time clustering~~
24 ~~parameters.~~ These changes suggest that previous methods may underpredict the number of Leak Indications (LIs) by 53.5%
25 with number of LIs detected in the old method being 27 and the new method detecting 58. The majority of these LIs were
26 found to be emitting in a leak rate category of 0 - 2 L min⁻¹. Source appointment was included as a core step within the
27 algorithm itself, this stage was shown to reduce the misassignment of LIs, suggesting the previous methodology may include
28 emissions from pyrogenics and biogenics within their LI assignments. ~~When source appointment was included as a core step~~

29 within the algorithm itself, the total fugitive natural gas emissions within a city was reduced from 185.10 L min⁻¹ to 60.23 L
30 min⁻¹, nearly three times lower.

31 1 Introduction

32 Following COP26 and the methane pledge (*European Commission and United States of America 2021*), methane and its
33 emissions have received increased attention. The pledge states that the signatories will attempt to reduce their methane
34 emissions by 30% of their 2020 levels by 2030. ~~This and~~ was brought about due to increasing concern over the potency of
35 methane as a greenhouse gas. With a warming potential 28 times greater than CO₂ over a 100-year timescale and 84 times
36 higher over a 20-year timescale (*IPCC, 2021*).

37 65 % of all methane emissions are thought to be anthropogenic in nature and atmospheric methane has seen a consistent growth
38 rate of > 5 ppb year⁻¹ since 2007, with 2021 and 2022 seeing growth rates of 17.8 ppb year⁻¹ and 14 ppb year⁻¹ respectively
39 (Saunois et al., 2025), therefore understanding and mitigating anthropogenic methane is a key goal to comply with the global
40 methane pledge.

41
42 Of the anthropogenic emissions, the agricultural sector has the largest contribution towards atmospheric emissions (Saunois et
43 al., 2025). Although there are means of reducing the emissions from these areas, including changing cattle, crop or land
44 management as well as changing the feedstock of the cattle, for example grass silage to maize silage (Bačėninaitė et al., 2022;
45 Nisbet et al., 2025), these changes may still require time to implement, so this sector cannot be the sole focus in order to reach
46 the 2030 deadline. Although the growth rate of methane concentrations in the atmosphere has slowed since the 1980s, it is still
47 responsible for 20% of the warming caused by long-lived greenhouse gases since pre-industrial times (Kirschke et al., 2013).
48 The difficulty in reducing methane emissions is in part due to the wide range of emission sources, both natural and
49 anthropogenic. 60% of methane emissions are thought to be anthropogenic in nature (Karakurt et al., 2013, Saunois et al.,
50 2020) and of those emissions, by far the largest contribution arises from the agricultural sector with the two main areas of this
51 being enteric fermentation from ruminant livestock like cattle and emissions from paddy fields (Karakurt et al., 2013, Yusuf
52 et al., 2012). Although there are means of reducing the emissions from these areas, such as changing the feedstock of the cattle,
53 for example grass silage to maize silage (Bačėninaitė et al., 2022), there is still a requirement for social change and land
54 management change, both of which are difficult to implement for a 2030 deadline.

55 After agriculture the largest contribution to anthropogenic emissions is from the energy sector with oil, natural gas and coal
56 having relatively similar contributions to methane emissions. Natural gas is of particular importance to the UK, with it being
57 the 19th largest country emitter of methane from the natural gas network (*Scarpelli et al., 2022*).

58 One of the sources of methane emissions from the natural gas network is fugitive emissions. A fugitive emission is an
59 unexpected or unwanted emission of gas from a pressurised network that is not detected by standard means (*Sotoodeh, 2021*).

60 Within the natural gas network, they are commonly referred to colloquially as “Gas Leaks”, however the stigma surrounding

61 this term, both from industrial operators and the public, means the term fugitive emission is preferable to be used where
62 possible.

63 In the United Kingdom in 2023, 63.5 billion cubic metres of natural gas was consumed (*Energy Institute, 2024*). This is used
64 in a range of applications including industrial use, electricity generation and domestic use. Of ~~the UKs~~the UKs natural gas
65 consumption, 33.8 % is from the domestic sector (*DESNZ, 2024*), with 73.8 % of households in England and Wales using
66 mains gas for either heating or cooking purposes. (*Stewart et al., 2024*), in 2022 it was estimated that 117 kT of methane was
67 emitted as a result of fugitive emissions related to natural gas distribution (*NAEI, UK Emissions Data Selector*).

68 Within the UK, after natural gas is either produced or imported, it is first transported through the National Gas' National
69 Transmission System (NTS).The natural gas network consists of production or importing of natural gas; transport of high-
70 pressure natural gas through the National Gas' National Transmission System (NTS), a network of over 5,000 miles of high-
71 pressure steel pipes and more than 500 above ground installations. This natural gas is then transported by one of several of the
72 UK's Gas Distribution Networks (GDNs), a GDN first reduces the pressure from the NTS then oversees the pipework for pre-
73 meter distribution of natural gas to homes and businesses.; and finally, distribution of natural gas to homes and businesses
74 which occurs through the 4 Gas Distribution Networks (GDNs) in the UK.

75 ~~A GDN first reduces the pressure from the NTS before then supplying natural gas to its customers.~~ The GDN responsible for
76 York covers 2.7 million homes and businesses not just across Yorkshire, but also the northeast of England and northern
77 Cumbria, which means the operation of tens of thousands of kilometres of pipework. This all leads to many unknowns in the
78 locations of fugitive emissions. To combat this, many previous studies have implemented mobile measurement approaches
79 centred around the detection of areas with elevated methane.

80 1.1 Previous Mobile Measurement Methodology

81 There have been many different approaches to designing an algorithm to detect fugitive emissions of natural gas, all of which
82 utilise detection of an enhancement in CH₄ concentrations, the major component of natural gas. These algorithms define an
83 enhancement based on whether CH₄ mixing ratios are higher than a certain value (*Phillips et al., 2016*), are above a certain
84 percentile in measured readings (*Hopkins et al., 2016, Chamberlain et al., 2016*) or by using an outlier detection model (*Keyes*
85 *et al., 2020*).

86 The paper upon which our methodology is based, (von Fischer et al., 2017), defines Observed Peaks (OPs) as methane
87 enhancements > 110% of a 2.5-minute rolling background of the mean CH₄ concentrations two minutes before and after each
88 measured point, and that they occur over less than 160 m ~~(von Fischer et al., 2017)~~. Enhancements occurring within 5 seconds
89 of each other are then grouped together. Mobile surveys ~~It is required that drives~~ are repeated multiple times and Leak
90 Indications (LIs) are determined after grouping OPs that occur within 20 m of one another and seeing which of these grouped
91 clusters contain OPs from separate ~~drives~~mobile surveys. The LIs are then quantified into emission rates in L min⁻¹, using an
92 equation derived from the results ~~from of~~ a controlled release experiment, shown in Equation 1.:

$$93 \quad (\text{release rate} / \text{L min}^{-1}) = 0.1178 + 0.08267 \times M - 0.005175 \times A + 0.08626 \times K \text{ (Eq. 1)}$$

126 Aerodyne Tuneable Infrared Laser Direct Absorption Spectrometer (TILDAS) Laser Trace Gas Analyser for measurements of
127 ethane (Yacovitch *et al.*, 2014). Measurements of ethane are calibrated using a three point calibration of a high standard of
128 ethane (17.5 ppb), medium (2.5 ppb) and a zero, where calibration standard concentrations were confirmed via GC-MS. For
129 each mobile survey drive a calibration is performed before and after the mobile survey drive itself, a linear regression is
130 performed to find the slope and intercept of the calibration concentrations versus measured concentrations. The average is
131 taken for the two calibrations to account for instrument drift during the sampling drive survey and the resulting equation,
132 Equation 4, is then used to apply a correction to ethane concentrations.

$$C_2H_6_{corrected} = C_2H_6_{uncorrected} \cdot m + c \text{ (Eq. 4)}$$

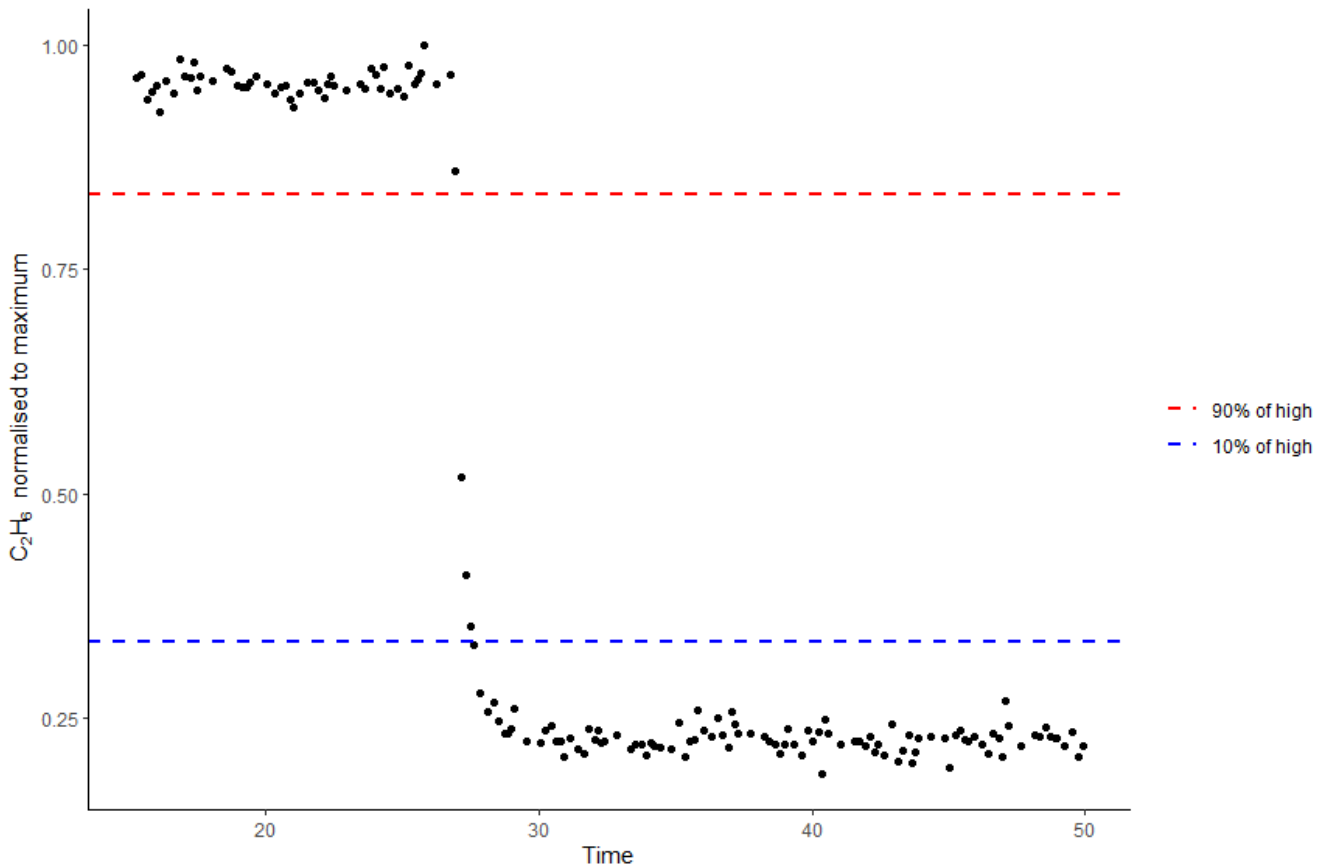
136 Where:

- 137 - m = Gradient of calibration concentration vs mean response averaged over the two calibrations
- 138 - c = Intercept of calibration concentration vs mean response averaged over the two calibrations

139 2.1.1 Instrument Response Time

140 Response time of the MGGA is reported as < 0.5 s from the manufacturer's specification. The response rate of the TILDAS
141 however was unknown. The TILDAS is capable of recording measurements at a rate of 10 Hz, however, the flow rate through
142 the instrument needed to be altered to make these measurements true to the 10 Hz values. Originally, the inlet to the TILDAS
143 had two valves in series, Stainless Steel Integral Bonnet Needle Valve, 0.37 Cv, 1/4 in. #SS-1RS4 and an electronic Upstream
144 Flow Control Valve, 10,000 sccm, 0.25 in. Tube, Viton Seal #0248A-10000SV which allows small changes to maintain the
145 internal pressure at 70 Torr. With the two valves in series, the instrument is unable to achieve a high enough flow rate for true
146 10 Hz measurements. Moving the valves to be parallel, the instrument was able to achieve a flow rate close to 5 Hz, at this
147 point it was found that the pump was the limiting factor for the flow rate of the instrument.

148 These changes to increase the flow rate of the instrument were made to allow for a response time as close to that of the MGGA
149 as possible. To find the accurate response time of the TILDAS, an experiment was devised whereby a high concentration of
150 ethane (17.630 ± 0.715 ppb, measured via GC-MS) was flowed through the TILDAS and switched to ambient air 10 times on
151 2 separate valve setups for a total of 20 repeats of low-high-low transitions in the concentration of ethane. The transition times
152 were located by eye and then the transition time to go from 90% of the maximum value to 10% of the maximum value was
153 calculated (Symonds, 2017), an example of the high to low transition with the 90 % and 10 % limits is shown in Figure 1.
154 The transition time on the first valve ranged from 0.7 – 1.1 s with a mean value of 0.9 s, the second valve having responses
155 ranging from 0.7 – 1.4 s also with a mean response of 0.9 s, giving confidence in a sub 1 s response rate from the TILDAS and
156 therefore showing the capability of a sub 1 s response in both instruments. The data however was still averaged to 1 s with a 1
157 s clustering time due to the data now being limited by the data acquisition rate of the WASP's GPS.



158 *Figure 1: Example response transition of TILDAS high concentration to low concentration, normalised to maximum*
 159 *recorded response*
 160
 161

162 **2.1.2 Variation in methane measurements**

163 Previous algorithms define an enhancement as being higher than 1.1 times a 2.5 minute rolling median background. This work
 164 however seeks to understand if this parameter holds true for the specific instrumentation used in the mobile surveys. To
 165 understand what this parameter may be, a variance experiment. The standard deviation of methane measurements over this
 166 period was calculated to understand the minimum detectable enhancement for the methane detection algorithm. For better
 167 understanding of minimum detectable enhancements of methane possible with the equipment available a variance experiment
 168 using compressed air flowing through the instrument for 2 hours. The standard deviation of methane measurements over this
 169 period was calculated to inform the enhancement criteria for the methane detection algorithm.

170 For 2 hours compressed air was flown through the Los Gatos MGGA, measured at a median value of 7.2 ppm, the standard
 171 deviation of these results was found to be 0.006 ppm. An enhancement criteria was proposed as ~~The enhancement criteria was~~

172 ~~calculated as~~ 5 times this standard deviation divided by the median baseline, ~~resulting in an enhancement criteria of in this~~
173 ~~ease~~ 1.005 times the baseline. However, this assumes a stable baseline that is replicated in the field. In reality, when applying
174 this enhancement criteria it leads to the detection of enhancements that are too small to be reliably quantified.

175 ~~Instead, the methane mixing ratios measured during each mobile survey, were collated and the standard deviation was~~
176 ~~calculated for each mobile survey. Again enhancement criteria was calculated as anything larger than 5 times the standard~~
177 ~~deviation divided by the median of methane mixing ratios, this was done for each mobile survey and resulted in a median~~
178 ~~enhancement criteria of 1.01 times the baseline. However as this would result in detection of enhancements that would be very~~
179 ~~small and could be diffuse or from enhancements that occurred far from the roads and therefore harder to quantify as true~~
180 ~~natural gas emissions, a larger enhancement criteria of 1.05 times the background was selected. This ensured there was still a~~
181 ~~large difference from the original methodologies criteria, while still remaining within the instrumentation known variation.~~
182 ~~Instead, the variation in the calculated baseline for drives was found and it was therefore determined that an enhancement of~~
183 ~~1.05 times the baseline should be used instead.~~

185 2.2 Driving Route

186 York is a city in the north-east of England with a population over 200,000. A driving campaign took place over two separate
187 weeks in May and June of 2024 resulting in 18 ~~drives~~ mobile surveys of a “flower petal” route, shown in *Figure 2*, staying
188 within the outer ring roads of the A64 and A1237 and mainly sampling residential areas of the city. ~~T~~he majority of the roads
189 sampled on the route were only driven in one direction but due to the position of the sampling inlet this allowed the middle of
190 the road to be ~~the~~ sampled ~~point~~ regardless of the direction of travel. The route was driven 18 times as, in order to capture
191 ~~number of times due to findings that to capture~~ > 90 % of emissions, a route should be driven at least 5 – 8 times over separate
192 days (*Luetschwager et al., 2021*). The route was chosen as it covers multiple different neighbourhoods within York, but was
193 not intended to be used to compare measurements to the cities emissions inventory due to only covering a small fraction of the
194 total miles of road within the York urban area, 27 miles of a total 507 administered by the local authority (*Department for*
195 *Transport, 2025*).

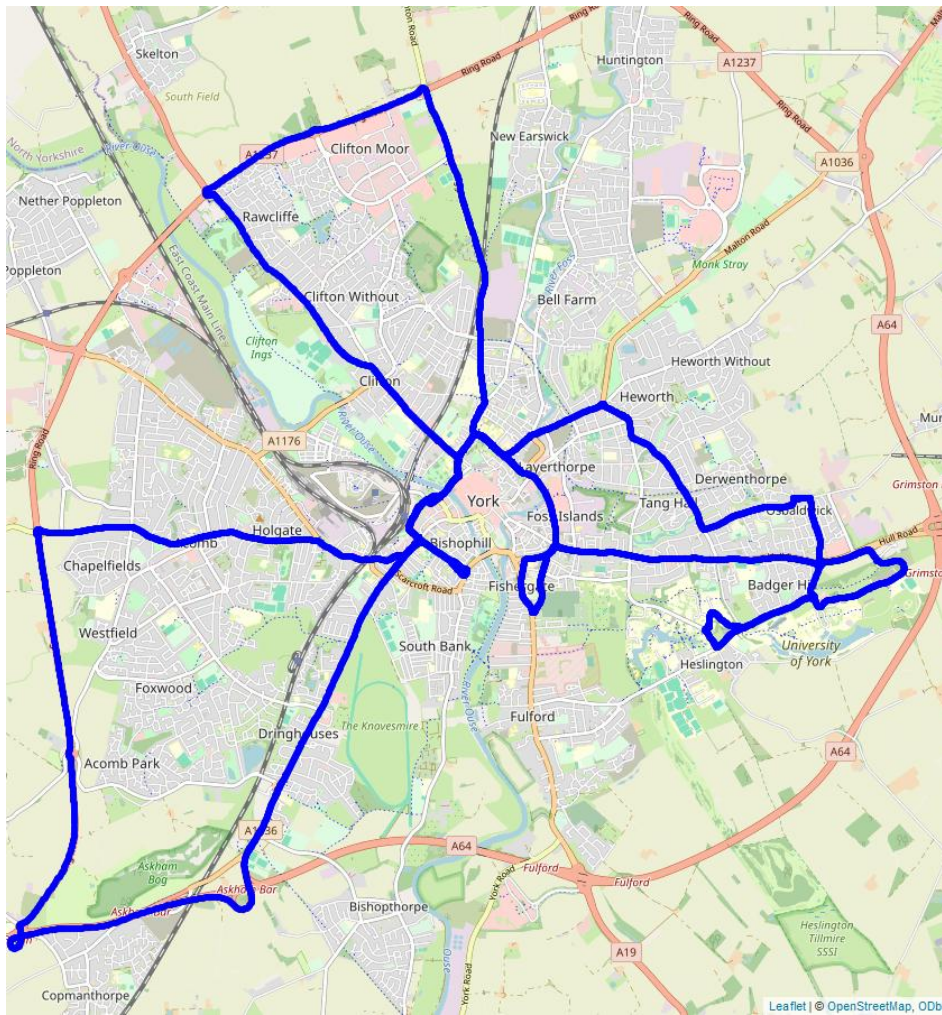


Figure 2: Map of the route taken in WASP surveys.

2.3 Enhancement Detection Algorithm

The original algorithm, used in (Weller et al., 2019), has been adapted following the findings in 2.1.1 and 2.1.2. OPs are clustered within 1 s as opposed to 5 s. With a faster instrument response, it was expected that the measurements would more readily distinguish between two separate enhancements that occurred spatially close to one another. By clustering over a time of 5 s, assuming an average speed of 20 miles per hour (8.9 m s^{-1}), this would mean the potential to cluster together enhancements 44.5m apart, whereas a cluster time of 1 s would at most be clustering enhancements 8.9 m apart, the reason for this change was discussed in 2.1.1. Enhancement criteria was also changed, instead of an enhancement needing to be more than 110 % of the baseline, it must be 105 % of the baseline. This allows detection of smaller enhancements, the change was discussed in 2.1.2. LI determination occurred after identifying the source type of each OP, ensuring LI analysis occurs only

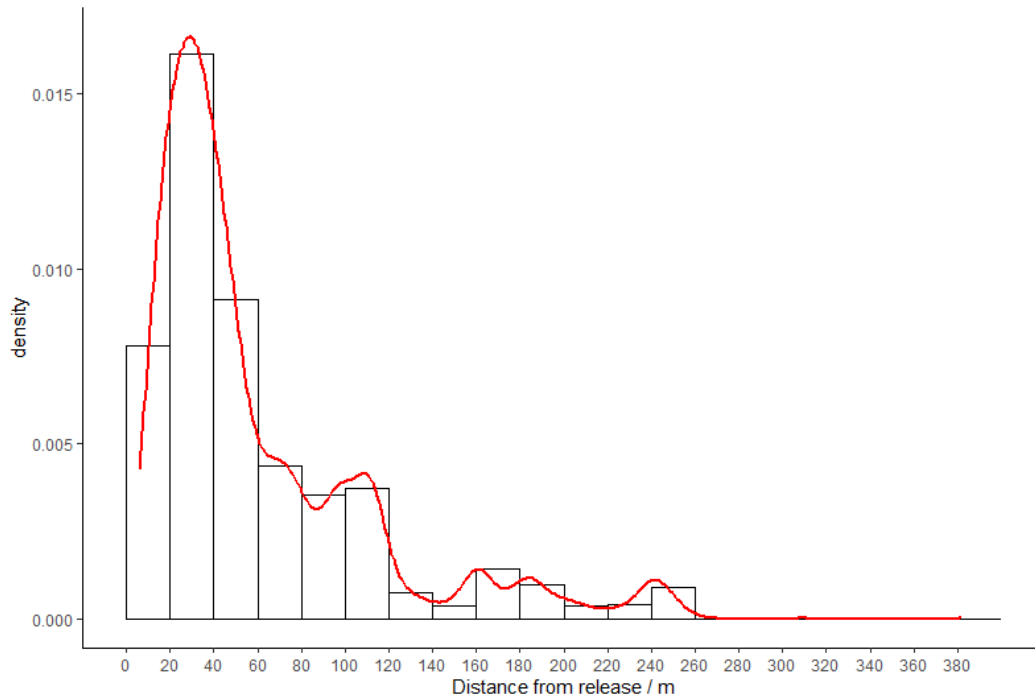
207 ~~on OPs of the same source type, to further reduce the chance of comparing long standing thermogenic fugitive emissions with~~
208 ~~possible nearby single occurrence pyrogenic or biogenic emissions. Unlike the previous iterations of the algorithm, OPs are~~
209 ~~clustered within 1 s as opposed to 5 s. With a faster instrument response, it was expected that the measurements would more~~
210 ~~readily distinguish between two separate enhancements that occurred spatially close to one another. Additionally, by clustering~~
211 ~~over a time of 5s, assuming an average speed of 20 miles per hour (8.9 m/s), this would mean the potential to cluster together~~
212 ~~enhancements 44.5m apart, whereas a cluster of 1s would at most be clustering enhancements 8.9 m apart, the reason for this~~
213 ~~change was discussed in 2.1.1. Enhancement criteria was also changed such that instead of an enhancement needing to be more~~
214 ~~than 110% of the baseline value to instead being an enhancement related to the results of the variance experiment to allow~~
215 ~~detection of smaller enhancements, this variation is discussed in 2.1.2. LI determination occurred after identifying the source~~
216 ~~type of each OP, to allow LI analysis to occur on OPs of the same source type, to further reduce the chance of comparing long~~
217 ~~standing thermogenic fugitive emissions with possible nearby single occurrence pyrogenic and biogenic emissions.~~

218 2.4 Controlled Release Experiment

219 To attain a quantification equation specific to the equipment used at York, a controlled release experiment was conducted at
220 the Bedford Aerodrome. The controlled release took place at the Bedford Aerodrome over 5 days in June of 2024. A MiniCRF
221 was deployed to manage releases of methane and ammonia, while a MidiCRF was deployed for releases of ethane. In total
222 there were 41 releases lasting an average of 30 minutes each. Releases consisted of varying amounts of methane (0.2 – 70.48
223 L min⁻¹), ethane (0 – 7.01 L min⁻¹) and ammonia (0 – 7.87 L min⁻¹) to reflect a range of methane sources, including natural gas
224 and farm emissions. Releases were from a mixture of linear vertical releases, a multi emission point ring, multi point source
225 emissions and single point releases, occurring at heights ranging from ground level to 3_m elevation. Over the course of the
226 experiment wind speeds were measured using four Gill Met Pak Pro instruments deployed at 3_m, 6_m, 9_m and 12 metres
227 elevation, winds were recorded as 1 minute vector averages. Average wind speed over the 5 days was 3.87 m s⁻¹ with wind
228 speeds ranging from 0 - 9.75 m s⁻¹. During each release, an initial period was spent locating the plume before sampling the
229 plume at set distances for 10 repeats ~~-, the platform then stepped before stepping~~ further away in distance for another set of 10
230 repeats, ~~-, this continued repeated~~ until the plume was either lost, or a lack of driveable ground was left available. ~~It~~ It was noted
231 that larger releases were detectable further away. ~~h~~ However, as the data from the controlled release was intended to be used
232 in quantifying sub-road and near-road fugitive emissions of natural gas, a maximum distance of 30_m from the controlled
233 release point was applied due to this reflecting the maximum road widths typically found within a city like York (*Essex*
234 *Planning Officers Association, 2018*).

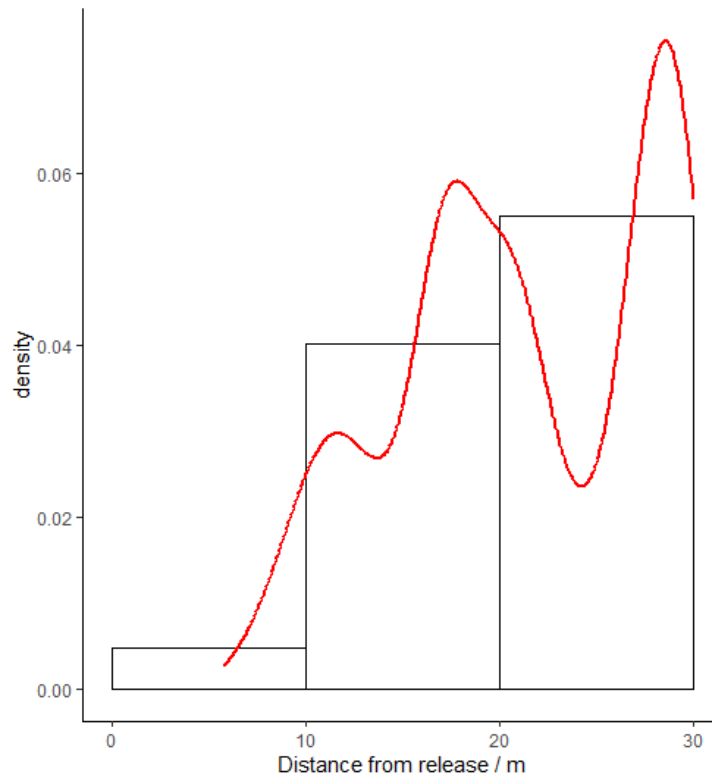
235
236 Of the 41 releases conducted in the controlled release, only 26 releases were able to be used for processing data, this is due to
237 several reasons, including some releases not having detectable enhancements. Within these 26 releases, 3525 methane
238 enhancements were detected over distances between 5.8 m and 382.1 m from the release point. ~~the majority of releases~~
239 detected further away from the release point were from higher emission rate releases. When this was filtered to include

240 enhancements from only 30 m from the release point this resulted in including 1226 enhancements from 23 drivesmobile
241 surveys. Density plots of number of detected enhancements against distance from source are shown in **Figure 3** for all detected
242 enhancements and **Figure 4** for enhancements detected within 30 m from the source.



243
244
245
246

Figure 3: Density plot of number of detected enhancements against distance from release point



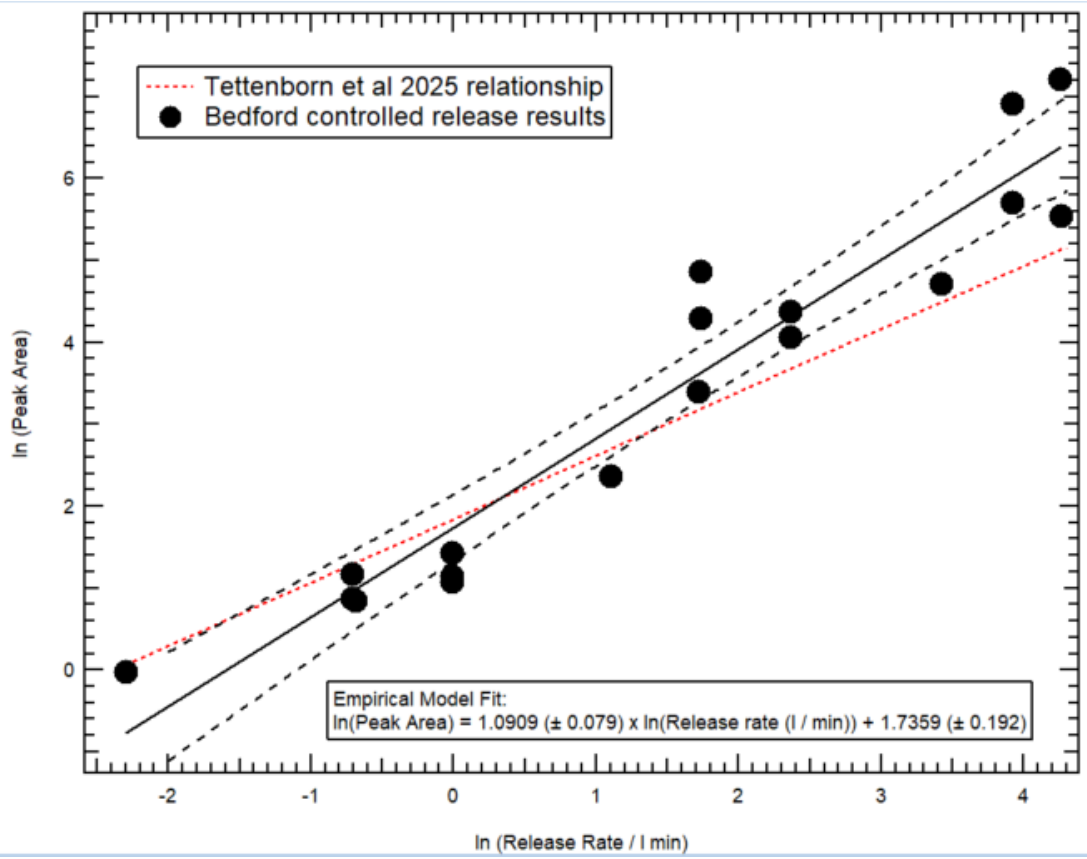
247 **Figure 4:** Density plot of number of detected enhancements against distance from release point (Limited to 0 – 30 m)

249 **2.4.1 Quantification equation**

250 There has been much development and advancement in the last few years on the use and application of “Advanced Mobile
 251 Leak Detection” systems for natural gas emissions detection and reporting. The original methodologies, where algorithms
 252 were developed to convert peak height maxima of measured methane plumes to estimated emission rates (Weller et al., 2019)
 253 have been superseded with plume area algorithms (Tettenborn et al. 2025) which are instrument and vehicle speed agnostic.
 254 However, this is still not a precise conversion, and can only be treated as a generalised guide to emissions estimation as factors
 255 such as wind, instrument inlet location and local variability due to buildings and unknown source locations.

256
 257 In order to reduce the uncertainty for the WASP as much as possible, we present the results of a 1-week controlled release
 258 experiment conducted under variable wind conditions in a simple open field environment. Whilst this does not replicate the
 259 complex conditions of an urban setting, previous work in (Tettenborn et al. 2025) shows that combined results from both urban
 260 and open field settings can be combined to give a generalised trend to create their plume area emission algorithm. For the
 261 WASP, the setup is slightly different to the work in (Tettenborn et al. 2025), with the WASP’s inlet located on the driver’s
 262 side at low elevation. This may influence the impact of vehicle turbulence on the measurements and the difference in elevation

263 will lead to a different vertical section of the plume being sampled. A comparison between the results of the York controlled
264 release, and the (Tettenborn et al. 2025) methodology averages are shown below in **Figure 5**. All data shown is for downwind
265 transects where the plume was intercepted at a maximum of 30 m from the controlled release location. The plume area is
266 calculated as a function of distance travelled (as opposed to time) to correct for vehicle speed differences as done in the original
267 (Tettenborn et al. 2025) work.



268 **Figure 5:** Peak area vs actual release rate for plume transects within 30m of release. Data shown is an average of multiple
269 transects (at least 10) for each release.

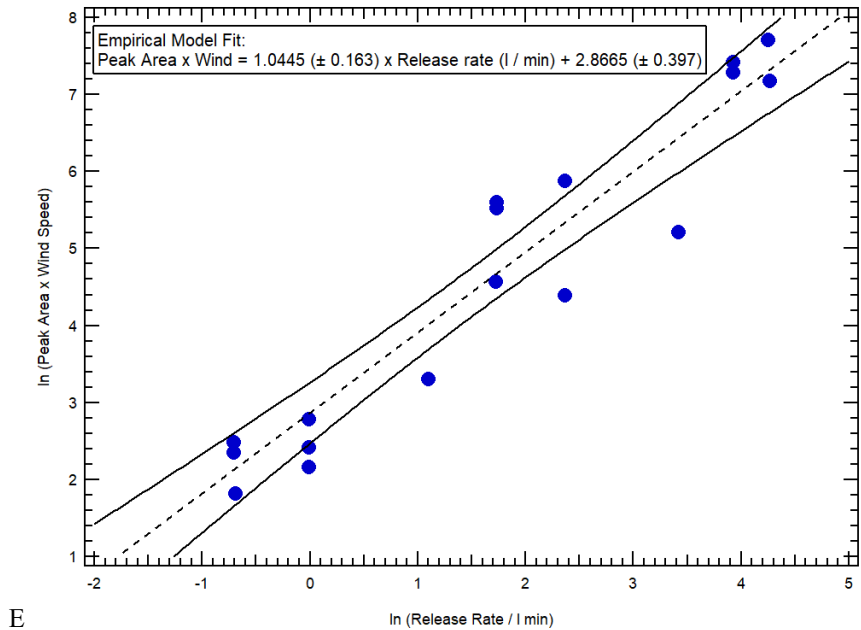
270
271
272 As it can be seen in **Figure 5**, whilst the general trend of increasing plume area with release rate is adhered to, the gradient of
273 the trend is steeper – implying that a near-ground based inlet is potentially more capable of ascribing differences in emission
274 rates.

275
276 One of the expected limitations of these algorithmic methods is the assumption that the effect of windspeed is ignored, which
277 given the importance of windspeed in more distal emissions modelling such as Gaussian plume modelling from vehicles (Dowd
278 et al. 2024) may be an oversight. Using the 3 m mast, 1 Hz wind data (averaged to 1 minute data) located on site at the

279 controlled release, the wind data is incorporated into the algorithm to give a volumetric correlation with the release rate
280 according to *Equation 5*.

$$281 \text{ wind speed} \times \int_{\text{plume start}}^{\text{plume end}} [\text{CH}_4] \text{ (Eq. 5)}$$

282 The results of the integration of the wind speed into the algorithm are shown below in *Figure 6*. Possibly somewhat
283 surprisingly, there is a slight decrease in the goodness of fit to the relationship – potentially due to plume dynamics close to
284 source not being immediately controlled by the atmospheric conditions, but the dynamics of the emission. This may also
285 provide evidence as to the reasons why the results of previous studies have ended up with metrics that would at first hand seem
286 unlikely to be able to produce reliable results from atmospheric dispersion principles. Given this result, that it seems to be as
287 robust to consider wind as to not, it may be prudent for future controlled release experiments to focus on recreating the
288 conditions of gas migration prior to emission to the atmosphere to see if this result still holds true.



289 ***Figure 6:*** Peak area x Wind speed vs actual release rate for plume transects within 30m of release. As with *Figure X*, data
290 shown is an average of multiple transects (at least 10) for each release.

291
292
293 Due to these findings, the quantification equation used within York mobile surveys is shown in *Equation 6*.

$$294 \ln(\text{release rate} / \text{L min}^{-1}) = 0.9167 \times \ln(\text{Peak Area}) - 1.7359 \text{ (Eq. 6)}$$

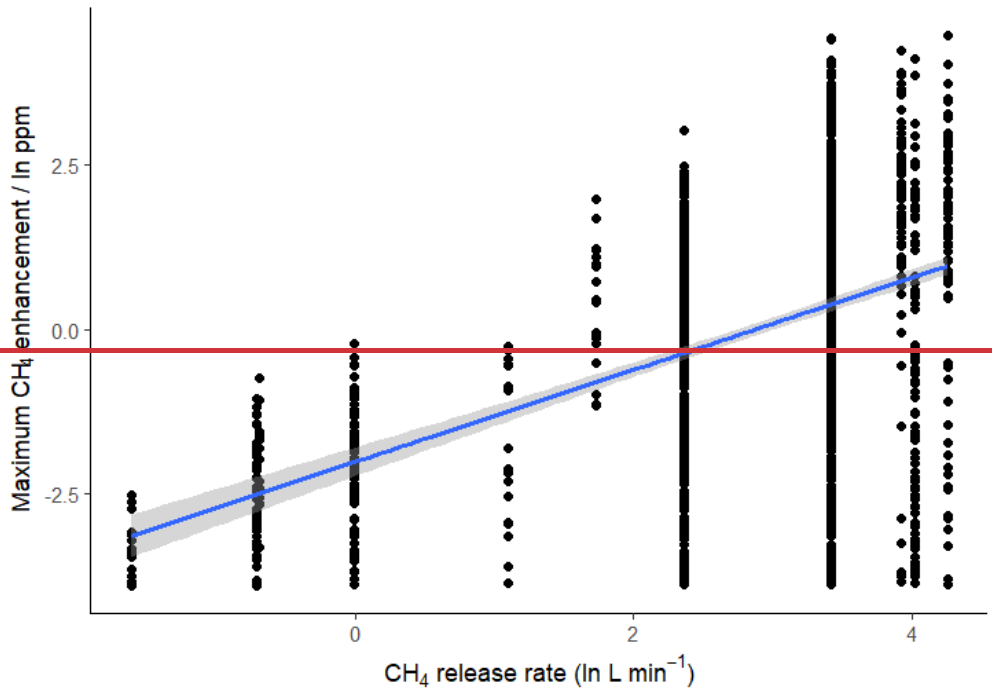
295 Additionally, leak rates were then reported within bins, similar to that within (*Tettenborn et al., 2025*), where three possible
296 bins were assigned: high ($> 40 \text{ L min}^{-1}$), medium ($6 - 40 \text{ L min}^{-1}$) and small ($< 6 \text{ L min}^{-1}$). This was adapted for the York
297 surveys, the small category was changed to $2 - 6 \text{ L min}^{-1}$ and a new category, very small, was introduced which contained leak

298 rates of 0 - 2 L min⁻¹. This change was introduced due to the lower enhancement criteria within the York methodology which
299 allows for detection of much smaller fugitive emissions.

301 It is important to note that these results are only suitable for the specific set up utilised here, and should not be more widely
302 applied without corroboration with other instruments or platform packages.

303 A quantification equation to calculate emission rate from CH₄ measurements could be calculated using enhancements that
304 were detected within 30 m of the controlled release emission point, to better reflect the enhancements likely to be detected
305 from under road natural gas emissions. By first using the methane detection algorithm a linear regression model could then
306 be used to find a relationship between the release rate and the maximum enhancement. 1226 enhancements were detected from
307 23 separate releases that were within 30 m of the emission point. These enhancements were determined from CH₄ releases
308 ranging from 0.49 to 70.48 L min⁻¹. A linear regression was then performed using the equation:

$$\ln(\text{maxexcess } CH_4) = b_0 + b_1 * \ln(\text{emission rate}) + \epsilon, \epsilon \sim \text{iid } N(0, \sigma^2)$$



311 **Figure 5:** Plot of the ln of the maximum detected CH₄ enhancement against the ln of the known CH₄ release rate.

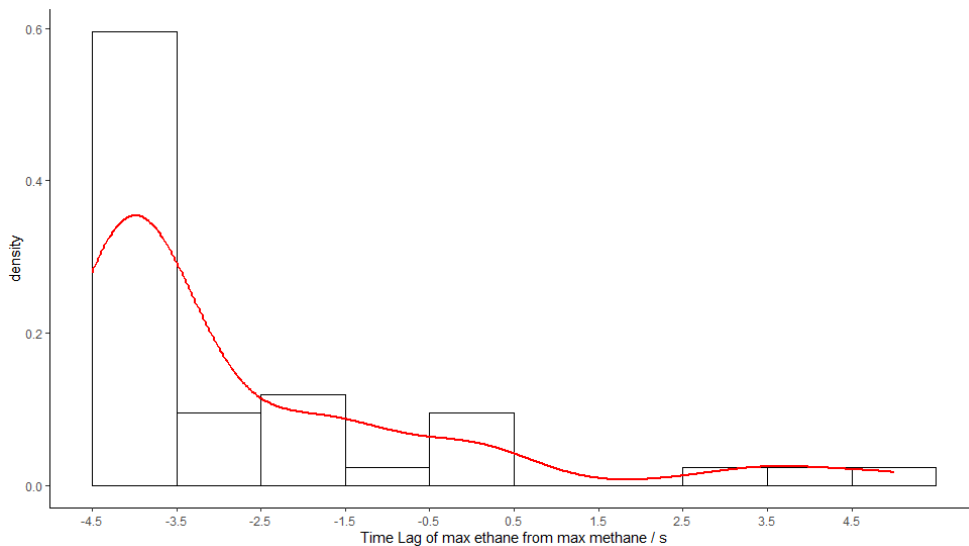
313 This resulted in the quantification equation;

$$\ln(\text{maxexcess } CH_4) = -1.2668 + 0.6323 * \ln(\text{emission rate}) -$$

316 **2.4.2 Instrument Lag Time**

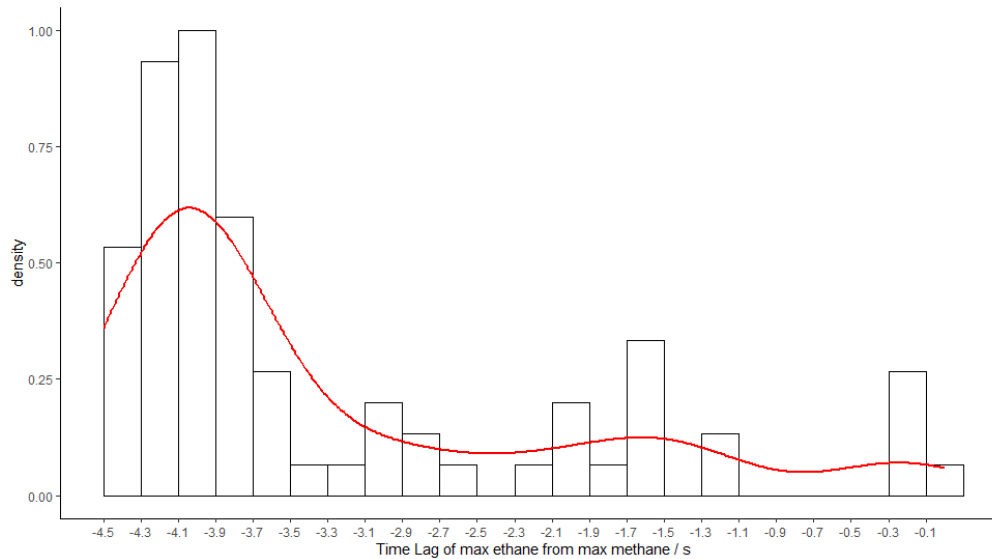
317 For each of the releases, the lag time between detecting an ethane enhancement and a methane enhancement was calculated.
318 With knowledge of Due to the response times of the instruments, it was expected that the TILDAS would respond to an
319 enhancement before the MGGA, however, this assumes that both instruments receive the same packet of air at the same time,
320 while, in reality, the packet of air will take a different amount of time to flow through manifold to each instrument. To find
321 this more accurate lag time of the instruments, the maximum methane enhancement for each pass was found, following this
322 the maximum ethane enhancement was found (that occurred within 5 seconds of the methane). The 5-resulting 10 second
323 window was selected as on transects of the controlled release the van travelled at roughly 20 miles hour⁻¹ph. Over the course
324 of 10 s (5_s either side of the methane maximum) this would mean 85 m covered in the van, the average length of a transect
325 being 180 m. The time lag between ethane and methane showed that in most cases (88.1_%), maximum ethane concentration
326 preceded maximum methane concentration with a mean lag of 2.7 s before and a median of 3.8 s before. Observing a window
327 of max methane to 5 s before max methane resulted in a mean lag of 3.3 s from ethane to methane and a median lag of 3.9 s.
328 This helped inform the detection algorithm to look for maximum ethane within a window only up to 5s before the maximum
329 methane. Density plots showing the time lag of maximum ethane from maximum methane are shown in Figure 7 for the full
330 10 second time window and Figure 8 for up to 5 seconds before the time of maximum measured methane.

331
332



333
334
335

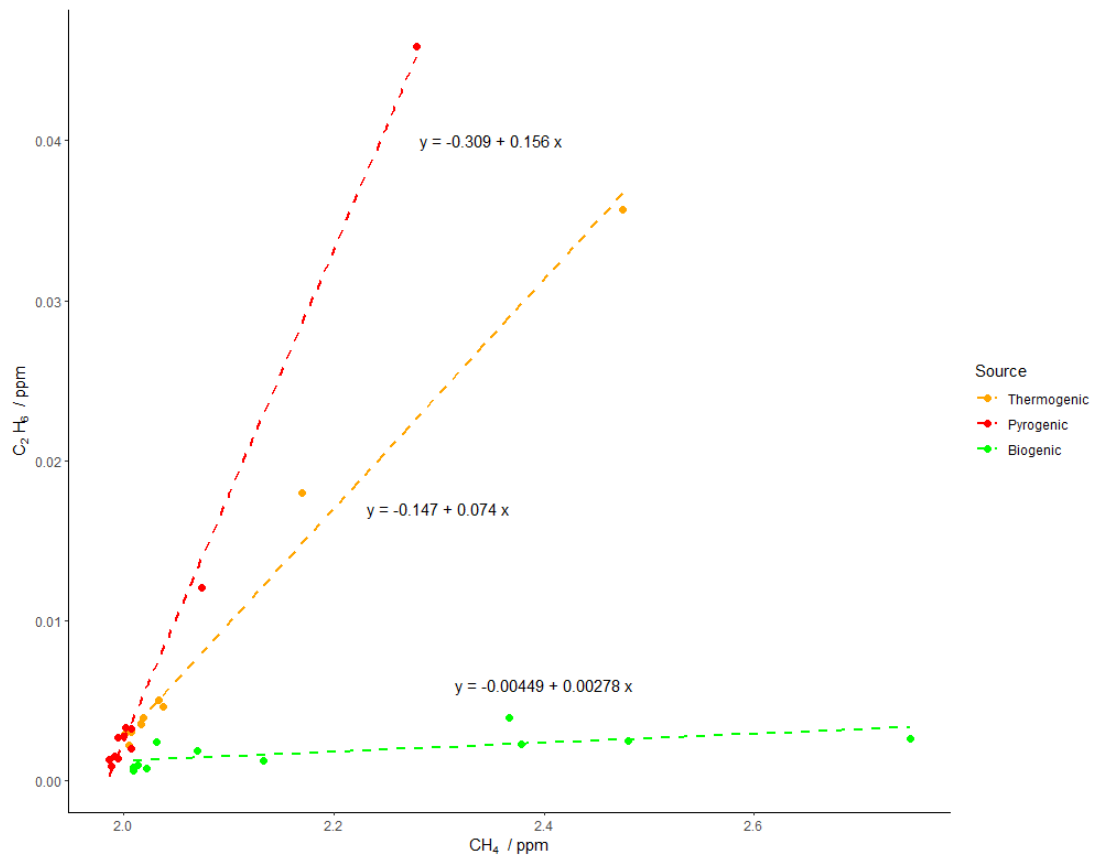
Figure 76: Density plot of time lag of the maximum ethane measurement from the maximum methane measurement.



336
 337 **Figure 78:** Density plot of time lag of the maximum ethane measurement from the maximum methane measurement (Only
 338 including ethane measurements that precede the methane)

339 2.5 Source Apportionment

340 Source determination using ethane-methane ratios has been shown to be effective, due in part to the knowledge that ethane is
 341 present in measurable quantities in thermogenic gas but not biogenic gas (Fernandez et al., 2022).²⁵ ethane:methane (C₂:C₁)
 342 ratios can be used in order to determine the source of a methane emission. Demonstrated in (Fernandez et al., 2022; Defratyka
 343 et al., 2021; Lowry et al., 2020; Yacovitch et al., 2014), C₂:C₁ < 0.005 ~~may be~~ associated with biogenic sources, > 0.005 to
 344 < 0.09 are thermogenic and > 0.1 are considered pyrogenic or combustion. Ideal examples of these relationships are shown in
 345 Figure 9. In order to calculate these ratios methane and ethane values must first be aligned in time. To complete this time
 346 alignment of methane and ethane values needs to be completed due to them being measured on separate instruments, the
 347 criterion for aligning these times is based on the results from 2.4.2. Additionally, enhancements are removed where the R² of
 348 CO₂:CH₄ is greater than 0.9 to ensure no combustion sources are wrongly assigned as thermogenic.



349
 350 **Figure 98:** Relationship between CH₄ and C₂H₆ for three OPs of different source types located during the sampling
 351 campaign.

352 **3 Results**

353 **3.1 Results of York ~~Drives~~mobile surveys**

354 17 ~~drives-mobile surveys~~ were conducted across the route of York, the raw data was taken from 10Hz files for methane
 355 (MGGGA) and ethane (TILDAS) and time averaged to 1_Hz data to be of the same response time as the WASPs other internal
 356 components (e.g. GPS). a colour map of the resulting measured methane concentration is shown in Figure 10. The data was
 357 then processed to remove data taken when speeds were 0 or > 40 miles hour⁻¹ph as well as removing data within the area of
 358 Wolfson Atmospheric Chemistry Laboratories due to this also being the location within which calibrations and other
 359 instrument tests were conducted. A rolling 2.5-minute median background of CH₄ was then taken-applied and enhancements
 360 were determined as any CH₄ measurement taken that was greater than 1.05 times the calculated background. The enhanced
 361 readings were then clustered such that any elevated reading within one second of another were assumed to correspond to the

379 ~~was determined using the equation present in 2.4.1 using the mean $\ln(\text{peak area})$ of all OPs within the LI cluster. The smallest~~
380 ~~leak rate was determined to be 0.0126 L min⁻¹ and the largest being 16.044.13 L min⁻¹. when assigned to bins 2 were small (2~~
381 ~~- 6 L min⁻¹) and 22 were very small (0 - 2 L min⁻¹).~~ When the source type filter is omitted, this results in 58 LIs with leak rates
382 ranging from 0.0124 to 23.104.70 L min⁻¹, when assigned to bins 9 were small (2 - 6 L min⁻¹) and 49 were very small (0 - 2 L
383 min⁻¹).~~In terms of cumulative leak rates, without source attribution cumulative leak rate would be 185.1 L min⁻¹ whereas when~~
384 ~~source attribution was factored in a cumulative leak rate of 60.2 L min⁻¹ was found.~~

385 3.1.1 Industry applicability

386 As many gas distribution companies have signed up to voluntary emission reporting programmes, such as the Oil and Gas
387 Methane Partnership (OGMP) 2.0, they are now obligated to report emissions through measurement based methods. One of
388 the most popular methods for such a reporting programme is through comprehensive, repeated vehicle based measurement
389 surveys of an operator's gas network. Here, we have a repeated route of measurements where thermogenic emissions have
390 been reported at certain locations throughout the campaign. It is therefore interesting from a mitigation perspective to
391 investigate how many times each of those thermogenic emissions were identified over the course of the campaign.

392

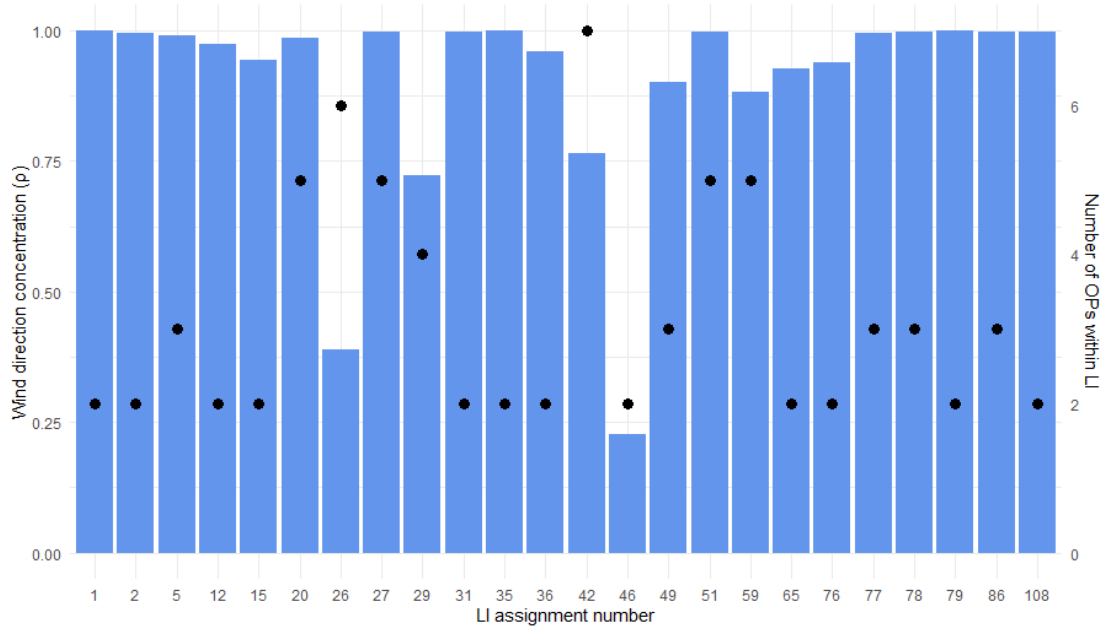
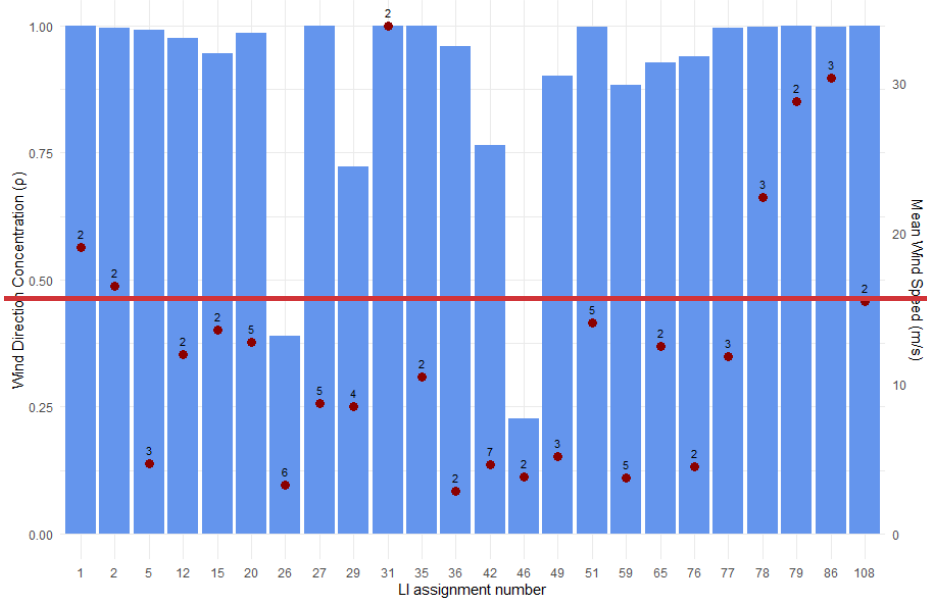


Figure 101: Wind direction consistency and and number of OPs ~~wind speed~~ per Thermogenic leak indication (Labelled with number of enhancements in each LI)

The effect of wind on detection of LIs was initially investigated by calculating the mean resultant length of wind directions when a Thermogenic OP was detected. This was calculated using Equation 7 ~~the equation:~~

400

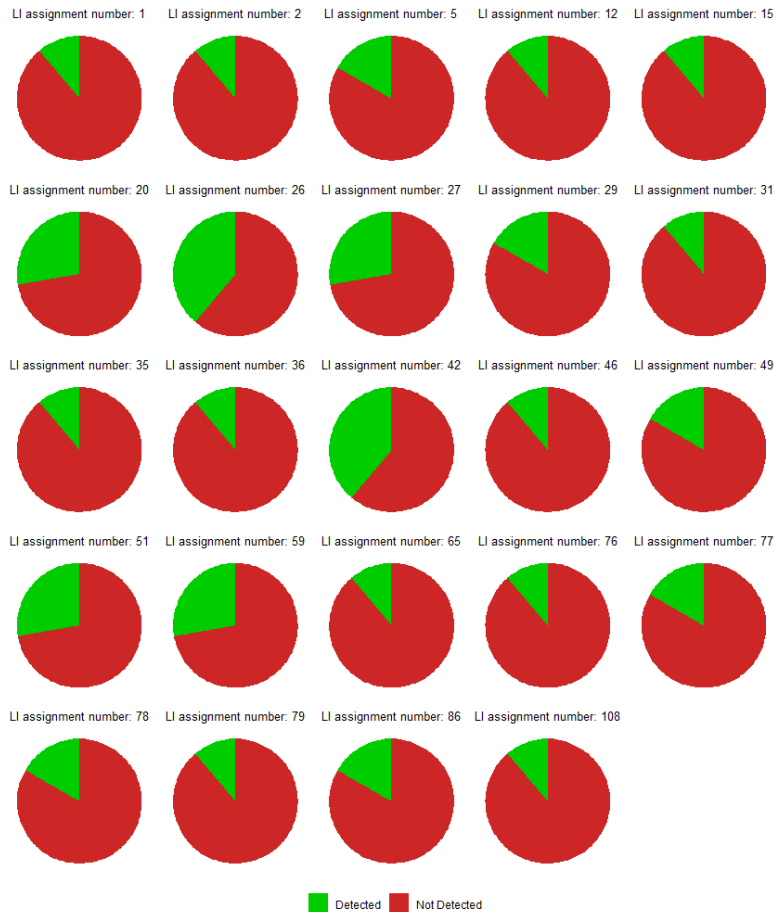
$$\rho = \frac{1}{n} \sqrt{\left(\sum_{i=1}^n \cos\theta_i\right)^2 + \left(\sum_{i=1}^n \sin\theta_i\right)^2} \text{ (Eq. 7)}$$

401 Where:

- 402 - ρ is mean resultant length
- 403 - n is number of data points
- 404 - θ_i is the angle in radians

405 For this analysis ρ is close to 1 when the wind directions are concentrated (similar) and close to 0 when more dispersed.

406 **Figure 10** shows that for the majority of LIs detected in York ρ is close to 1, suggesting that most LIs occur away from the
 407 road and require correct wind direction in order to detect them. ~~For LIs where ρ is lower it can also be noted that the mean
 408 wind speeds also tend to be lower, suggesting that these LIs may occur closer to the mobile platform therefore not needing a
 409 specific direction of wind in order to detect them.~~



410

411

Figure 12: Pie charts of each LI showing number of ~~drives-mobile surveys~~ they were detected vs not

412

413 ~~The number of mobile surveys drives~~ is a large factor in the probability of detecting an LI. Each LI requires the
414 enhancement to be detected on at least 2 separate ~~mobile surveys drives~~, for the 24 LIs detected over the course of this
415 campaign 12 LIs were detected on 2 drives, 6 were detected on 3 drives, 4 on 5 drives and 2 on 7, this meant that the average
416 probability of detection was 0.18. ~~detection versus non detection for each LI is demonstrated in Figure 12.~~ This low
417 probability of detection highlights the need for surveys with multiple passes.

418 **3.2 Emissions from other sources**~~Pyrogenic emissions~~

419 While 1778 of the 4687 OPs were determined to be Thermogenic, 3941 were assigned as biogenic (8.38%) ~~and 1996 were~~
420 Pyrogenic (41.82%) ~~and 53 were not able to be assigned a source type.~~ NO_x:CO₂ ratios were investigated for the pyrogenic
421 Ops these OPs using the same methodology used for the CH₄:C₂H₆ source assignment. 1152 of the 1996 pyrogenic OPs were
422 able to be analysed in this way, 875 of these 1152 OPs (75.9%) had a NO_x:CO₂ ratio < 0.88 x 10⁻³. This implied that the
423 majority of pyrogenic emissions did not originate from traffic but more likely emissions from domestic heat and power
424 generation (such as emissions from domestic boilers) (Cliff *et al.*, 2025). ~~When these 85 Pyrogenic boiler OPs were clustered~~
425 ~~over 30m and filtered to only include multiple drives (much like how LIs were determined from Thermogenic OPs) it resulted~~
426 ~~in only 5 recurring emissions of this type, this is to be expected, as emissions from boilers are less likely to be a consistent~~
427 ~~emission source than a fugitive emission from a natural gas pipe.~~

428 Emissions from pyrogenic sources are compared at the OP stage on a mobile survey by mobile survey drive by drive basis due
429 to the high unlikelihood of pyrogenics and biogenics being persistent emission sources, the number of times each source type
430 was detected per mobile survey is shown in Figure 13.~~these emissions being detected on multiple drives.~~

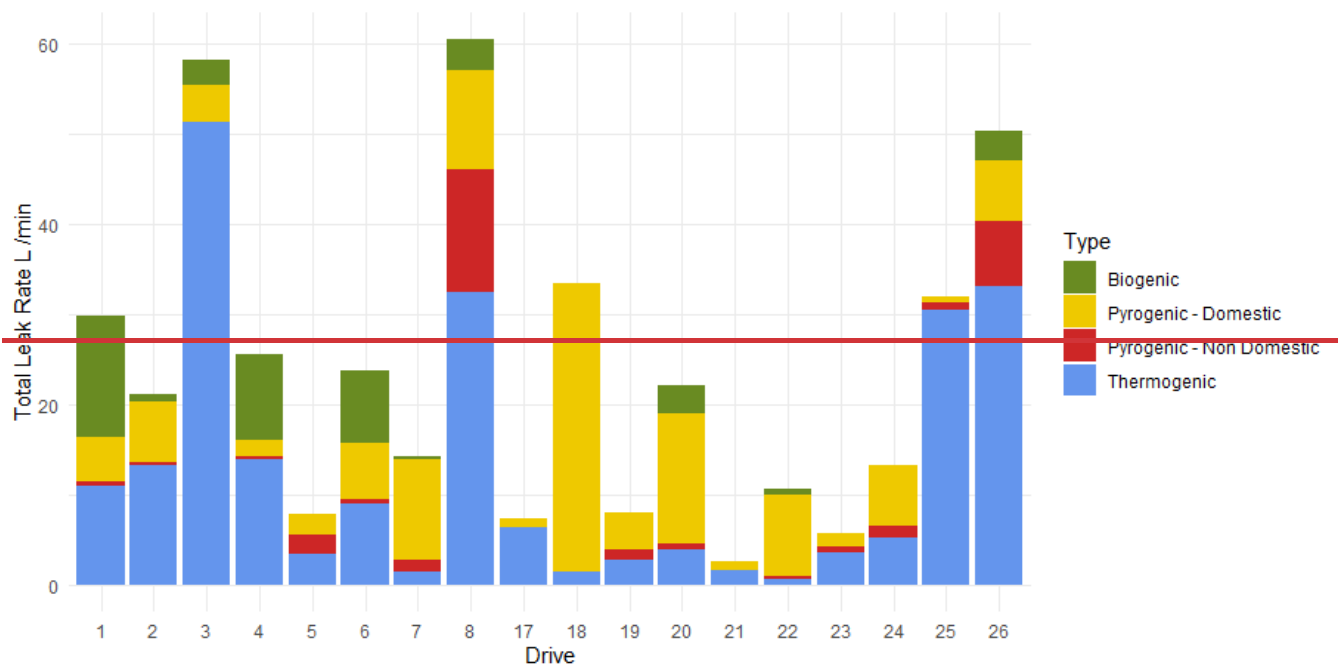


Figure 12: Total leak rate ($L \cdot min^{-1}$) contribution from each source type for each of the drives.

431
432
433

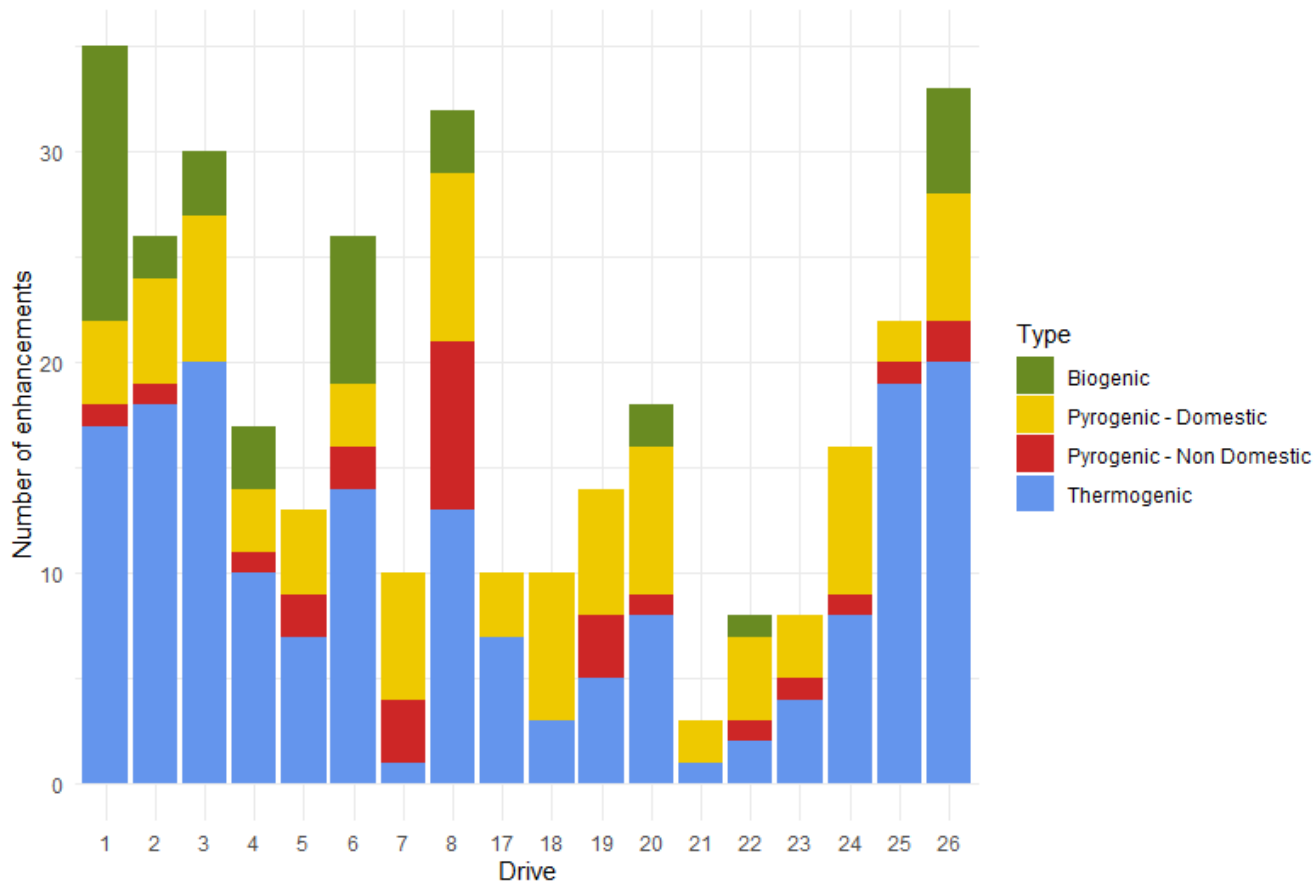


Figure 13: Total number of enhancements from each source type for each of the mobile surveys.

Thermogenics were the most frequently located source type on 13 of the 18 surveys, with mobile surveys 7, 18, 19, 21 and 22, finding pyrogenic emissions related to heating and cooking were the most frequently occurring source type. Thermogenic emissions from natural gas had the highest overall contribution to OPs across all drives and had the highest individual contribution on 10 of the 18 drives. However, for 7 of 18 drives pyrogenic emissions related to heating and cooking had the second highest overall contribution to methane emissions along the sampling route. For all source types, the majority of enhancements detected were of leak rates less than 5 L min^{-1} ; no non-domestic pyrogenic or biogenic emission was detected with a leak rate greater than 10 L min^{-1} . Although a few higher leak rate outliers were detected for domestic pyrogenics, thermogenic emissions were the only source type with emissions seen consistently at leak rates up to 20 L min^{-1} .

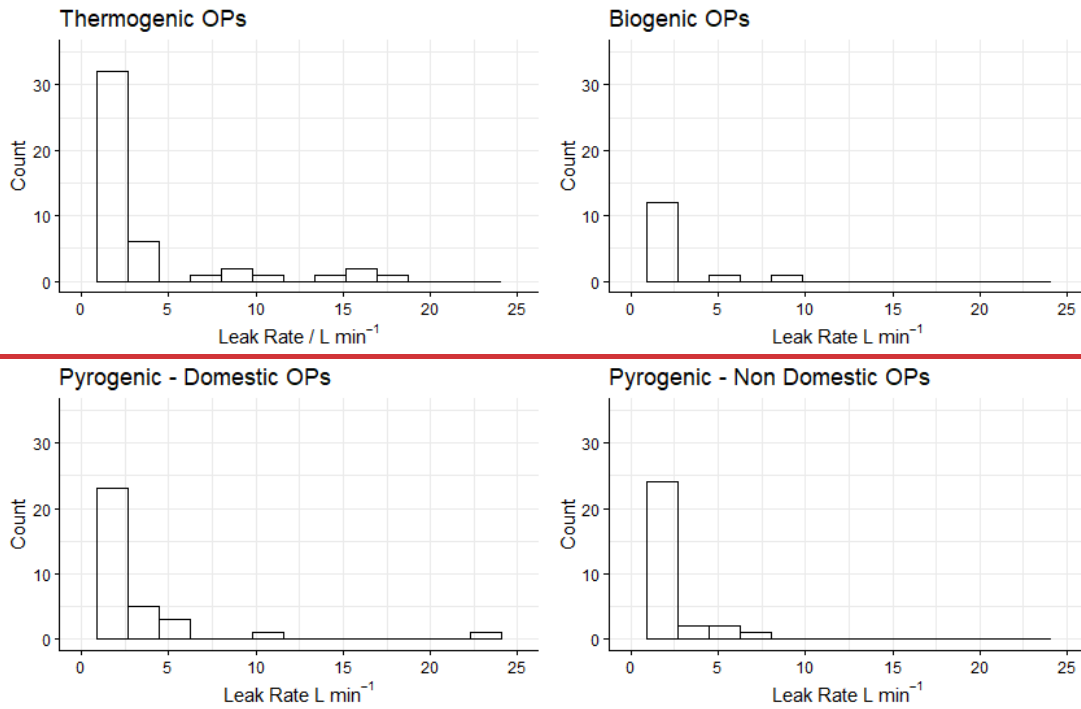


Figure 13: Histograms of leak rate distributions by source type.

3.3 Comparison to previous methods

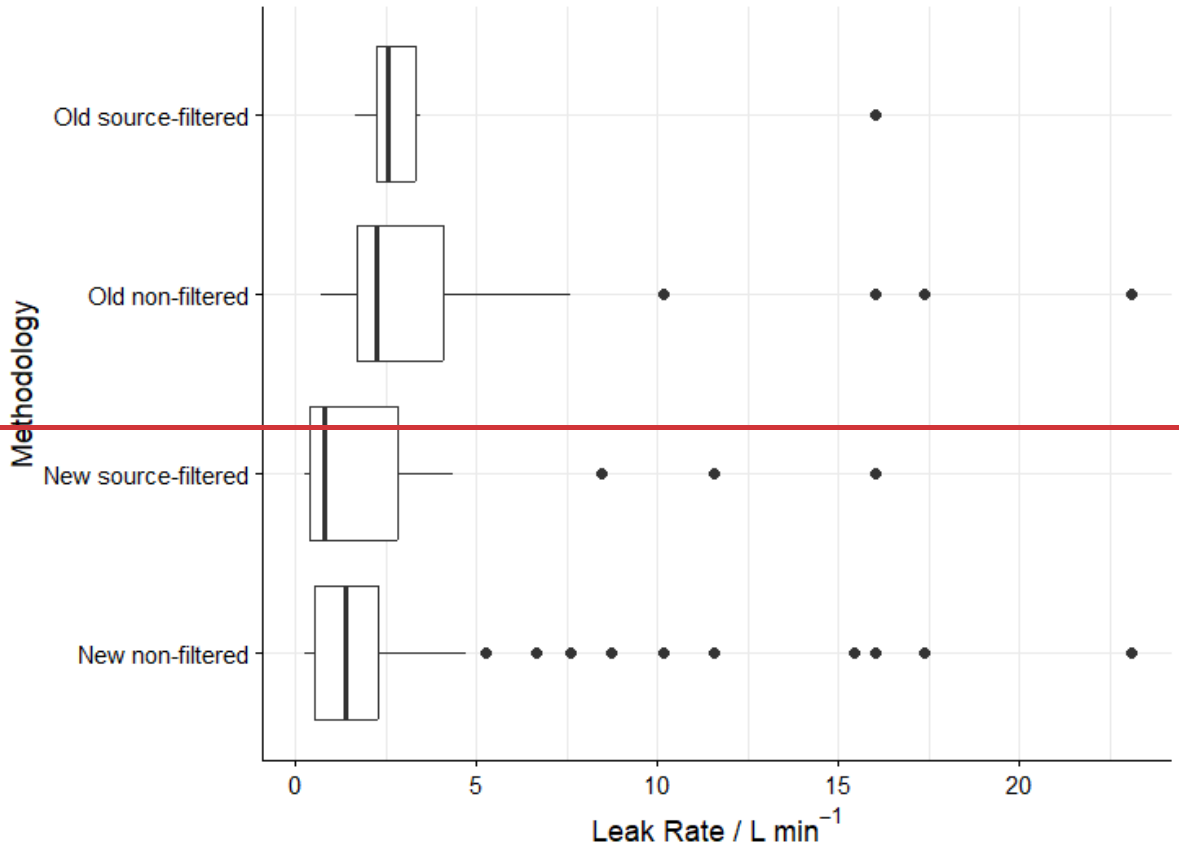
The main alterations to this methodology from that present in (Weller et al., 2019) (and other studies that were based of this method) were that enhancement criteria was changed from 1.1 times the baseline to 1.05 times the baseline, clustering by time was changed such that emissions within 1 s of each other were clustered instead of those within 5 s. F and finally that a source determination stage was added as a core step in the algorithm as opposed to previous iterations that either had no source determination stage or one that came later in the analysis. Table 1 shows the effect that all of these changes to the methodology make on the resulting detection of OPs and LIs. filter was applied as opposed to no source determination occurring or that this came later in the analysis. By comparing the methodology with the new one derived from the instrument limitations we find the following:

Enhancement Criteria	Time Clustering Criteria / s	Source Determination Included?	Number of OPs	Number of LIs
110% of baseline	5	No	179	27
		Yes	66	6
	1	No	216	29
		Yes	79	7
105% of baseline	5	No	357	58
		Yes	144	23
	1	No	46 8 7	58
		Yes	17 7 8	24

Table 1: Number of detected OPs and LIs depending on changing algorithm parameters

457
458
459 This shows Showing the new methodology could locate more LIs. Additionally, when the predicted leak rates were compared
460 from the non-source filtered LIs it showed that in addition to being able to locate more LIs, the changes to enhancement criteria
461 and time clustering have also led to the ability to locate LIs of a greater range of leak rates. Binning into the leak rate categories
462 of very small (0 - 2 L min⁻¹), small (2 - 6 L min⁻¹), medium (6 - 40 L min⁻¹) and high (> 40 L min⁻¹) showed that of the 24 LIs
463 in the new source filtered methodology, 2 were small and 22 were very small. For the 58 LIs of the new non filtered
464 methodology, 9 were small and 49 were very small. For the previous method the = 27 detected = from the old non filtered
465 methodology 10 were small and 17 were very small. LIs range in leak rate between 0.70 and 23.10 L min⁻¹, with a mean Leak
466 Rate of 4.53 L min⁻¹, 75% of LIs have a leak rate between 1.71 and 4.10 L min⁻¹, whereas with the new enhancement criteria
467 and time clustering parameter there was a range in leak rate of 0.24 to 23.10 L min⁻¹, a mean of 3.19 L min⁻¹ and 75% of LIs
468 having a Leak rate between 0.51 and 2.26 L min⁻¹. The total methane emissions from LIs were 122.43 L min⁻¹ for the old
469 method compared to 185.10 L min⁻¹ for the new method. This however changes when the source filtering is factored in where
470 the Leak Rates ranged from 0.26 to 16.04 L min⁻¹ with a mean leak rate of 2.51 L min⁻¹ and 75% of LIs having a leak rate
471 between 0.38 and 2.85 L min⁻¹ additionally the cumulative emissions was 60.23 L min⁻¹. If this source filtering is applied to
472 the old method however we see that for the 6 LIs, leak rates ranged from 1.64 to 16.04 L min⁻¹ with a mean of 4.74 L min⁻¹
473 and a cumulative emission of 28.48 L min⁻¹. Showing the old methods underprediction in total methane emissions of 33.9%
474 when not source filtered and 59.4% when source filtering is considered. Finally the 6 LIs from the old source filtered
475 methodology, 1 was small and 5 were very small. This shows the old methodology requiring an enhancement of 1.1 times the
476 baseline with 5 s time clustering misses a large proportion of LIs that the newer methodology, requiring an enhancement of

477 1.05 times the baseline with 1 s time clustering, detects. A large proportion of these missed LIs occur in the very small category
478 as expected with a smaller enhancement criteria. Source filtering shows that regardless of criteria used less LIs will be detected
479 with this method, this suggests previous methodologies that do not use this stage may be mischaracterising some thermogenic
480 enhancements as being permanent as they may instead be detecting methane enhancements of differing source types that occur
481 within the same vicinity of one another.

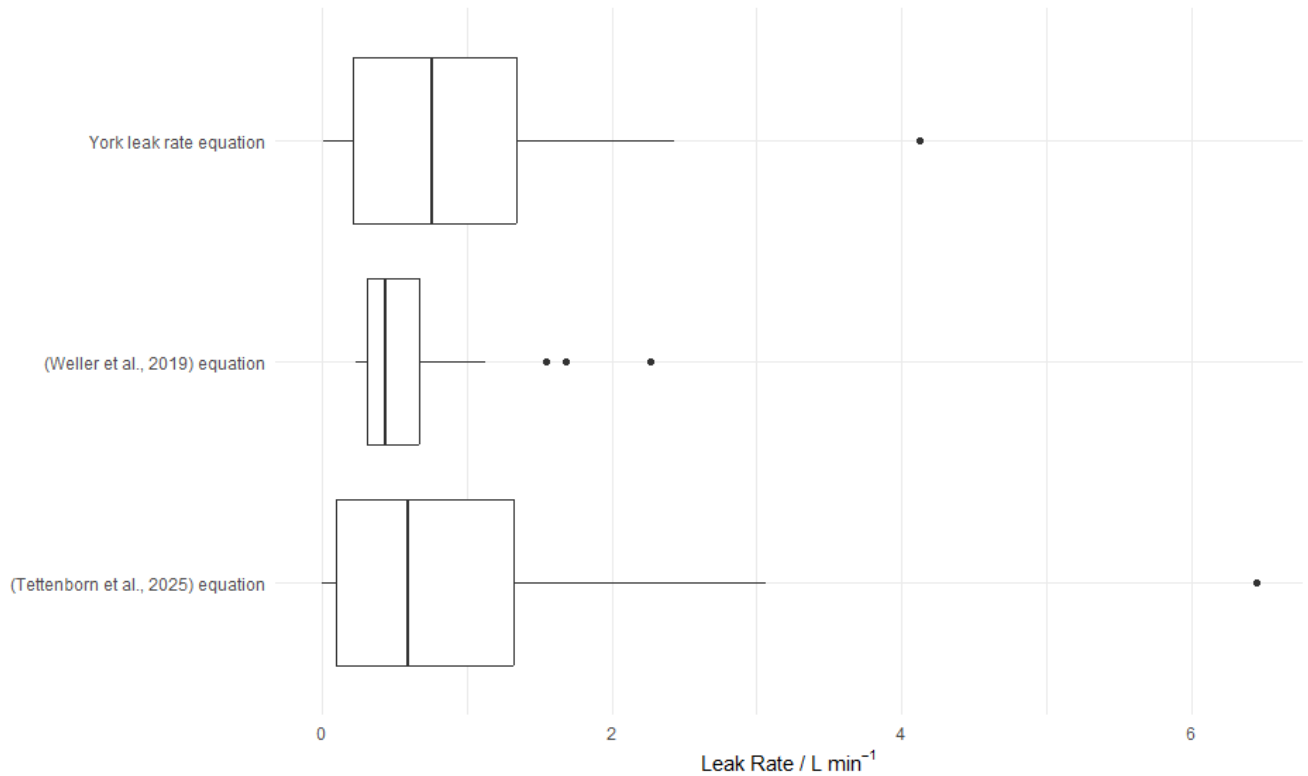


483 *Figure 14: Box plot showing the varying detected Leak Rates depending on methodology used*

485 3.4 Comparison of alternate quantification approaches

486 As previously described, the quantification equation used within this body of work is based on the (Tettenborn et al., 2025)
487 approach of using peak area to calculate the leak rate of a LI. However, previous works have used the quantification equation
488 present in (Weller et al., 2019) which instead quantifies release rate based on peak height. This campaign's results were
489 reprocessed using each of these previous quantification equations in order to compare the effects of the updated parameters in
490 the York quantification equation to the original, present in (Tettenborn et al., 2025) but also to explore the difference in

491 quantified leak rates from a peak height approach. As previously mentioned, the results of the York quantification approach
492 resulted in the 24 LIs being assigned to leak rate bins such that 2 were small and 22 were very small, the (Tettenborn et al.,
493 2025) equation results in 1 medium, 1 small and 22 very small and the (Weller et al., 2019) equation results in 1 small and 23
494 very small. The specific leak rates of LIs calculated with these three equations are presented in box-plots in **Figure 14.**



495 **Figure 14: Comparison of calculated leak rates of LIs from each of the 3 quantification equations.**

496 This shows that both the peak area approaches result in a much larger range of calculated leak rates from the LIs than from the
497 peak height approach present in (Weller et al., 2019). This suggests that the instrumentation used to detect CH₄ enhancements,
498 may result in low, wide peaks as opposed to higher, sharper peaks, thus explaining why leak rates are weighted much lower
499 from this method. The (Tettenborn et al., 2025) equation appears to be mostly consistent with the equation determined from
500 the York methodology, however there is slightly higher weighting of leak rates with the (Tettenborn et al., 2025) equation,
501 resulting in the 24 LIs changing from the assignments of 5 small and 19 to 1 medium, 5 small and 18 very small.
502
503

504 4. Conclusions

505 This study focused on using the specifications of the equipment used for the surveying to better inform a detection algorithm.
506 Enhancement criteria was determined by investigating the variance of the MGGA, although laboratory experiments
507 suggested the instrumentation was capable of detecting enhancements at a minimum of 1.005 times the baseline was possible,
508 in field experiments showed that enhancement criteria of 1.01 times the baseline was more likely the lower limit for
509 detection. However, for the surveys a criteria of 1.05 was selected so as to not incorporate small, diffuse emissions within the
510 analysis., in field experiments showed that a preferable limit was 1.05 times the baseline. Response rate of the instruments
511 was calculated to inform the time window for clustering, with both MGGA and TILDAS having sub one second response
512 rate, the time clustering was instead limited to one second due to the limitations of GPS data collection speed.
513 These changes show previous methodologies would result in detection of 27 LIs compared to the 58 LIs using updated
514 parameters (53.5 % less), the parameter change has also shown the ability to detect more LIs in all leak rate categories, but in
515 particular, the very small (0 - 2 L min⁻¹) category, where 17 of 27 LIs were located in the previous methodology, but 46 of
516 the 58 were located in the new methodology.
517 ~~These changes show previous methodologies would result in detection of 33.9% lower cumulative emissions.~~
518 Source appointment proved to be a useful tool for predicting emissions directly related to natural gas, when source filtering
519 was introduced at the OP stage of detection, it resulted in only 41.4% of LIs still being detected as opposed to the non-source
520 filtered method. ~~Additionally, this meant a reduction of 67.5% in the total estimated emissions of methane.~~
521 Additionally source filtering has helped to highlight that although Thermogenic emissions from natural gas are the highest
522 contributor to methane emissions, pyrogenic emissions related to domestic heat and power generation also provide a high but
523 often overlooked contribution to a ~~cities~~city's methane emissions.
524 The updating of the quantification equation from a peak height approach to a peak area approach results in a much wider
525 range of leak rates being calculated in the study, however these values are not as high as when quantified using the original
526 equation presented in (Tettenborn et al., 2025).
527 This new method has shown that with changing enhancement criteria and time clustering parameters, it is able to detect
528 many more LIs and a wider range of leak rates and that by applying a source type filter at the OP detection stage it is capable
529 of reducing of reducing the incorrect assignment of LIs, the overprediction of methane emissions from natural gas. However,
530 the methodology has ability to improve further, primarily by using instrumentation that is capable of detecting methane and
531 ethane on one instrument, so as to remove uncertainty related to time lag between the two instruments, but secondly by
532 having all instrumentation and hardware able to operate at a sub one second time rate in order to reduce the time clustering
533 parameter limit and further improve spatial resolution.

534 Code / Data availability

535 Code and data will be made available upon request.

536 **Author Contribution**

537 Contributed to conception: TM, JH, WD, JL. Contributed to data acquisition: TM, JH, WD, SY, SHB, MS, JL. Contributed to
538 analysis and interpretation of data: TM, JH, WD, SY, [MLV](#), JF, JL. Drafted and/or revised the paper: TM, JH, WD, SY, DL,
539 JF, JL. Approved the submitted version of this paper for publication: TM, JH, WD, SY, SHB, MS, JF, DL, JL.

540 **Competing Interests**

541 The authors declare that they have no conflict of interest.

542 **Acknowledgements**

543 We would like to thank the INGENIOUS (Understanding the sourceS, traNsformations and fates of IndOor air pollUtantS)
544 project, NERC grant number NE/W002256/1, for providing access to their data in the early stages of the method development.
545 Additionally we would like to thank both the National Physical Laboratory (NPL) and the MOMENTUM (Mobile
546 Observations and quantification of Methane Emissions to inform National Targeting, Upscaling and Mitigation) project, NERC
547 grant number NE/X014649/1, for organising and providing access to the controlled release experiment.

548 **References**

549 Ars, S., Vogel, F., Arrowsmith, C., Heerah, S., Knuckey, E., Lavoie, J., Lee, C., Pak, N.M., Phillips, J.L. and Wunch, D.,
550 Investigation of the spatial distribution of methane sources in the greater Toronto area using mobile gas monitoring systems.
551 Environ. Sci. Technol., 54(24), pp.15671-15679. <https://doi.org/10.1021/acs.est.0c05386>, 2020.
552
553 Bačėninaitė, D., Džermeikaitė, K. and Antanaitis, R., Global warming and dairy cattle: How to control and reduce methane
554 emission. Animals, 12(19), p.2687. <https://doi.org/10.3390/ani12192687>, 2022.
555
556 Chamberlain, S.D., Ingraffea, A.R. and Sparks, J.P., Sourcing methane and carbon dioxide emissions from a small city:
557 Influence of natural gas leakage and combustion. Environ. Pollut., 218, pp.102-110,
558 <https://doi.org/10.1016/j.envpol.2016.08.036>, 2016.
559
560 Cheng J, Schloerke B, Karambelkar B, Xie Y, Aden-Buie G. *leaflet: Create Interactive Web Maps with the JavaScript*
561 *'Leaflet' Library*. R package version 2.2.3.9000, <https://rstudio.github.io/leaflet/>, 2025
562

563 Cliff, S.J., Drysdale, W., Lewis, A.C., Møller, S.J., Helfter, C., Metzger, S., Liddard, R., Nemitz, E., Barlow, J.F. and Lee, J.
564 D., Evidence of Heating-Dominated Urban NO_x Emissions. Environ. Sci. Technol. 59(9), pp.4399-4408.
565 <https://doi.org/10.1021/acs.est.4c13276>, 2025
566
567 Defratyka, S.M., Paris, J.D., Yver-Kwok, C., Fernandez, J.M., Korben, P. and Bousquet, P., Mapping urban methane sources
568 in Paris, France. Environ. Sci. Technol., 55(13), pp.8583-8591. <https://doi.org/10.1021/acs.est.1c00859>, 2021
569
570 Department for Energy Security and Net Zero (DESNZ), Energy Trends: Natural Gas, Energy Trends September 2024,
571 https://assets.publishing.service.gov.uk/media/66f423473b919067bb48270e/Energy_Trends_September_2024.pdf (accessed
572 December 2024), 2024
573
574 Department for Transport: Road Length Statistics, RDL0102: Road length (miles) by road type and local authority in Great
575 Britain, <https://www.gov.uk/government/statistical-data-sets/road-length-statistics-rdl> (accessed April 2025), 2025
576
577 [Dowd, E., Manning, A.J., Orth-Lashley, B., Girard, M., France, J., Fisher, R.E., Lowry, D., Lanoisellé, M., Pitt, J.R.,
578 Stanley, K.M., O'Doherty, S., Young, D., Thistlethwaite, G., Chipperfield, M.P., Gloor, E. and Wilson, C., First validation
579 of high-resolution satellite-derived methane emissions from an active gas leak in the UK. Atmos. Meas. Tech., 17\(5\),
580 pp.1599–1615. <https://doi.org/10.5194/amt-17-1599-2024>, 2024.](#)
581
582 Energy Institute, Statistical Review of World Energy, Natural gas consumption in the United Kingdom (UK) from 2003 to
583 2023 (in billion cubic meters),
584 https://www.energyinst.org/_data/assets/pdf_file/0004/1055542/EI_Stat_Review_PDF_single_3.pdf (accessed December
585 2024), 2023.
586
587 Essex Planning Officers Association, The Essex Design Guide, Design Details, 2018 Edition, V3,
588 <https://www.essexdesignguide.co.uk/media/2402/design-details-v3.pdf> (Accessed December 2024), 2018.
589
590 European Commission, United States of America, Global methane pledge,
591 <https://www.ccacoalition.org/sites/default/files/resources//Global%20Methane%20Pledge.pdf> (accessed July 2025), 2021
592
593 Fernandez, J.M., Maazallahi, H., France, J.L., Menoud, M., Corbu, M., Ardelean, M., Calcan, A., Townsend-Small, A., van
594 der Veen, C., Fisher, R.E. and Lowry, D., Street-level methane emissions of Bucharest, Romania and the dominance of
595 urban wastewater. Atmos. Environ-X, 13, p.100153. <https://doi.org/10.1016/j.aeaoa.2022.100153>, 2022.
596

597 Hopkins, F. M.; Kort, E. A.; Bush, S. E.; Ehleringer, J. R.; Lai, C. T.; Blake, D. R.; Randerson, J. T. Spatial patterns and
598 source attribution of urban methane in the Los Angeles Basin. *J. Geophys. Res.: Atmos.* 121 (5), 2490– 2507,
599 <https://doi.org/10.1002/2015JD024429>, 2016.

600

601 IPCC, 2021: Climate Change 2021: The Physical Science Basis. Contribution of Working Group I to the Sixth Assessment
602 Report of the Intergovernmental Panel on Climate Change [Masson-Delmotte, V., P. Zhai, A. Pirani, S.L. Connors, C. Péan,
603 S. Berger, N. Caud, Y. Chen, L. Goldfarb, M.I. Gomis, M. Huang, K. Leitzell, E. Lonnoy, J.B.R. Matthews, T.K. Maycock,
604 T. Waterfield, O. Yelekçi, R. Yu, and B. Zhou (eds.)]. Cambridge University Press, Cambridge, United Kingdom and New
605 York, NY, USA, In press, <https://doi.org/10.1017/9781009157896>., 2021.

606

607 ~~Joo, J., Jeong, S., Shin, J. and Chang, D.Y., Missing methane emissions from urban sewer networks. *Environ. Pollut.*, 342,
608 p.123101. <https://doi.org/10.1016/j.envpol.2023.123101>, 2024.~~

609

610 ~~Karakurt, I., Aydin, G. and Aydiner, K., Sources and mitigation of methane emissions by sectors: A critical review. *Renew.*
611 *Energ.*, 39(1), pp.40–48. <https://doi.org/10.1016/j.renene.2011.09.006>, 2012.~~

612

613 Keyes, T., Ridge, G., Klein, M., Phillips, N., Ackley, R. and Yang, Y., An enhanced procedure for urban mobile methane
614 leak detection. *Heliyon*, 6(10). <https://doi.org/10.1016/j.heliyon.2020.e04876>, 2020.

615

616 ~~Kirschke, S., Bousquet, P., Ciais, P., Saunois, M., Canadell, J.G., Dlugokencky, E.J., Bergamaschi, P., Bergmann, D., Blake,
617 D.R., Bruhwiler, L. and Cameron-Smith, P., Three decades of global methane sources and sinks. *Nat. Geosci.*, 6(10), pp.813–
618 823. <https://doi.org/10.1038/ngeo1955>, 2013.~~

619

620 Lowry, D., Fisher, R. E., France, J. L., Coleman, M., Lanoisellé, M., Zazzeri, G., Nisbet, E. G., Shaw, J. T., Allen, G., Pitt,
621 J., and Ward, R. S.: Environmental baseline monitoring for shale gas development in the UK: Identification and geochemical
622 characterisation of local source emissions of methane to atmosphere, *Sci. Total Environ.*, 708, 134600,
623 <https://doi.org/10.1016/j.scitotenv.2019.134600>, 2020

624

625 Luetschwager, E., von Fischer, J.C. and Weller, Z.D., Characterizing detection probabilities of advanced mobile leak
626 surveys: Implications for sampling effort and leak size estimation in natural gas distribution systems. *Elem. Sci. Anth.*, 9(1),
627 p.00143. <https://doi.org/10.1525/elementa.2020.00143>, 2021.

628

629 Maazallahi, H., Fernandez, J.M., Menoud, M., Zavala-Araiza, D., Weller, Z.D., Schwietzke, S., Von Fischer, J.C., Denier
630 Van Der Gon, H. and Röckmann, T., Methane mapping, emission quantification, and attribution in two European cities:

631 Utrecht (NL) and Hamburg (DE). *Atmos. Chem. Phys.*, 20(23), pp.14717-14740. [https://doi.org/10.5194/acp-20-14717-](https://doi.org/10.5194/acp-20-14717-2020)
632 [2020](https://doi.org/10.5194/acp-20-14717-2020), 2020.

633

634 National Atmospheric Emissions Inventory (NAEI), UK Emissions Data Selector,
635 <https://naei.energysecurity.gov.uk/data/data-selector> . Selected emissions data for the year 2022, methane emissions related
636 to gas leakage from gas distribution 1B2b5. (accessed June 2025)

637

638 [Nisbet, E.G., Manning, M.R., Lowry, D., Fisher R.E., Lan, X., Michel, S.E., France, J.L., Nisbet, R.E.R, Bakkaloglu, S.,](#)
639 [Leitner, S.M., Brooke, C., Röckmann, T., Allen, G., Denier van der Gon, H.A.C, Merbold, L., Scheutz, C., Woolley Maisch,](#)
640 [C., Nisbet-Jones, P.B.R., Alshalan, A., Fernandez, J.M. and Dlugokencky, E.J., Practical paths towards quantifying and](#)
641 [mitigating agricultural methane emissions. *Proceedings of the Royal Society A: Mathematical, Physical and Engineering*](#)
642 [Sciences](#), 481, 20240390, <https://doi.org/10.1098/rspa.2024.0390>, 2025

643

644 Phillips, N.G., Ackley, R., Crosson, E.R., Down, A., Hutyra, L.R., Brondfield, M., Karr, J.D., Zhao, K. and Jackson, R.B.,
645 Mapping urban pipeline leaks: Methane leaks across Boston. *Environ. Pollut.*, 173, pp.1-4.
646 <https://doi.org/10.1016/j.envpol.2012.11.003>, 2013.

647

648 [Saunois, M., Martinez, A., Poulter, B., Zhang, Z., Raymond, P. A., Regnier, P., Canadell, J. G., Jackson, R. B., Patra, P. K.,](#)
649 [Bousquet, P., Ciais, P., Dlugokencky, E. J., Lan, X., Allen, G. H., Bastviken, D., Beerling, D. J., Belikov, D. A., Blake, D.](#)
650 [R., Castaldi, S., Crippa, M., Deemer, B. R., Dennison, F., Etiope, G., Gedney, N., Höglund-Isaksson, L., Holgerson, M. A.,](#)
651 [Hopcroft, P. O., Hugelius, G., Ito, A., Jain, A. K., Janardanan, R., Johnson, M. S., Kleinen, T., Krummel, P. B., Lauerwald,](#)
652 [R., Li, T., Liu, X., McDonald, K. C., Melton, J. R., Mühle, J., Müller, J., Murguia-Flores, F., Niwa, Y., Noce, S., Pan, S.,](#)
653 [Parker, R. J., Peng, C., Ramonet, M., Riley, W. J., Rocher-Ros, G., Rosentreter, J. A., Sasakawa, M., Segers, A., Smith, S. J.,](#)
654 [Stanley, E. H., Thanwerdas, J., Tian, H., Tsuruta, A., Tubiello, F. N., Weber, T. S., van der Werf, G. R., Worthy, D. E. J., Xi,](#)
655 [Y., Yoshida, Y., Zhang, W., Zheng, B., Zhu, Q. and Zhuang, Q., Global Methane Budget 2000 - 2020. *Earth Syst. Sci. Data*,](#)
656 [17, 1873-1958, https://doi.org/10.5194/essd-17-1873-2025, 2025.](#)~~[Saunois, M., Stavert, A.R., Poulter, B., Bousquet, P.,](#)~~
657 ~~[Canadell, J.G., Jackson, R.B., Raymond, P.A., Dlugokencky, E.J., Houweling, S., Patra, P.K. and Ciais, P., The global](#)~~
658 ~~[methane budget 2000–2017. *Earth Syst. Sci. Data*, pp.1–136. https://doi.org/10.5194/essd-12-1561-2020, 2019.](#)~~

659

660 Scarpelli, T.R., Jacob, D.J., Grossman, S., Lu, X., Qu, Z., Sulprizio, M.P., Zhang, Y., Reuland, F., Gordon, D. and Worden,
661 J.R., Updated Global Fuel Exploitation Inventory (GFEI) for methane emissions from the oil, gas, and coal sectors:

662 evaluation with inversions of atmospheric methane observations. *Atmos. Chem. Phys.*, 22(5), pp.3235-3249.
663 <https://doi.org/10.5194/acp-22-3235-2022>, 2022.

664

665 Sotoodeh, K., Why packing adjustment cannot stop leakage: Case study of a ball valve failing to seal after packing
666 adjustment during fugitive emission as per ISO 15848–1. *Eng. Fail. Anal.*, 130, p.105751.
667 <https://doi.org/10.1016/j.engfailanal.2021.105751>, 2021.

668

669 Stewart I., Bolton P.; Households off the gas-grid and prices for alternative fuels; House of Commons Library,
670 <https://researchbriefings.files.parliament.uk/documents/CBP-9838/CBP-9838.pdf> (accessed December 2024), 2024.

671

672 Symonds, J, August 15 2017, On Instrument Time Response: What it means, what it isn't, and why it matters, [Article],
673 LinkedIn. <https://www.linkedin.com/pulse/instrument-time-response-what-means-why-matters-jonathan-symonds/>
674 (Accessed November 2024)

675

676 [Tettenborn J., Zavala-Araiza D., Stroeken, D., Maazallahi, H., van der Veen, C., Hensen, A., Velzeboer, I., van den Bulk, P.,
677 Gillespie, L., Ars, S., France, J., Lowry, D., Fisher, R. and Röckmann, T., Improving consistency in methane emission
678 quantification from the natural gas distribution systems across measurement devices. *Atmos. Meas. Tech.*, 18, 3569–3584,
679 <https://doi.org/10.5194/amt-18-3569-2025>, 2025](https://doi.org/10.5194/amt-18-3569-2025)

680

681 [Ueyama, M., Umezawa, T., Terao, Y., Lunt, M. and France, J.L., Evaluating urban methane emissions and their attributes in
682 a megacity, Osaka, Japan, via mobile and eddy covariance measurements. *Atmos. Chem. Phys.*, 25\(19\), pp.12513–12534.
683 <https://doi.org/10.5194/acp-25-12513-2025>, 2025.](https://doi.org/10.5194/acp-25-12513-2025)

684

685 [Umezawa, T., Terao, Y., Ueyama, M., Kameyama, S., Lunt, M. and France, J.L., Measurement report: Mobile measurements
686 to estimate urban methane emissions in Tokyo. *Atmos. Chem. Phys.*, 25\(23\), pp.18015–18029. \[https://doi.org/10.5194/acp-
25-18015-2025\]\(https://doi.org/10.5194/acp-
687 25-18015-2025\), 2025.](https://doi.org/10.5194/acp-25-18015-2025)

688

689 Vogel, F., Ars, S., Wunch, D., Lavoie, J., Gillespie, L., Maazallahi, H., Röckmann, T., Nećki, J., Bartyzel, J., Jagoda, P. and
690 Lowry, D., Ground-Based Mobile Measurements to Track Urban Methane Emissions from Natural Gas in 12 Cities across
691 Eight Countries. *Environ. Sci. Technol.*, 58(5), pp.2271-2281. <https://doi.org/10.1021/acs.est.3c03160>, 2024.

692

693 von Fischer, J.C., Cooley, D., Chamberlain, S., Gaylord, A., Griebenow, C.J., Hamburg, S.P., Salo, J., Schumacher, R.,
694 Theobald, D. and Ham, J., Rapid, vehicle-based identification of location and magnitude of urban natural gas pipeline
695 leaks. *Environ. Sci. Technol.*, 51(7), pp.4091-4099. <https://doi.org/10.1021/acs.est.6b06095>, 2017.

696

697 Wagner, R. L., Farren, N. J., Davison, J., Young, S., Hopkins, J. R., Lewis, A. C., Carslaw, D. C., and Shaw, M. D.:
698 Application of a mobile laboratory using a selected-ion flow-tube mass spectrometer (SIFT-MS) for characterisation of
699 volatile organic compounds and atmospheric trace gases, *Atmos. Meas. Tech.*, 14, 6083–6100, [https://doi.org/10.5194/amt-](https://doi.org/10.5194/amt-14-6083-2021)
700 [14-6083-2021](https://doi.org/10.5194/amt-14-6083-2021), <https://doi.org/10.5194/amt-14-6083-2021>, 2021.

701

702 Weller, Z.D., Yang, D.K. and von Fischer, J.C., An open source algorithm to detect natural gas leaks from mobile methane
703 survey data. *PLoS One*, 14(2), p.e0212287. <https://doi.org/10.1371/journal.pone.0212287>, 2019.

704

705 Weller, Z.D., Im, S., Palacios, V., Stuchiner, E. and von Fischer, J.C., Environmental injustices of leaks from urban natural
706 gas distribution systems: patterns among and within 13 US metro areas *Environ. Sci. Technol.*, 56(12), pp.8599-8609.
707 <https://doi.org/10.1021/acs.est.2c00097>, 2022.

708

709 Wietzel, J.B. and Schmidt, M., Methane emission mapping and quantification in two medium-sized cities in Germany:
710 Heidelberg and Schwetzingen. *Atmos. Environ-X*, 20, p.100228. <https://doi.org/10.1016/j.aecaoa.2023.100228>, 2023.

711

712 Yacovitch, T.I., Herndon, S.C., Roscioli, J.R., Floerchinger, C., McGovern, R.M., Agnese, M., Pétron, G., Kofler, J.,
713 Sweeney, C., Karion, A. and Conley, S.A., Demonstration of an ethane spectrometer for methane source
714 identification. *Environ. Sci. Technol.*, 48(14), pp.8028-8034. <https://doi.org/10.1021/es501475q>, 2014.

715

716 ~~Yusuf, R.O., Noor, Z.Z., Abba, A.H., Hassan, M.A.A. and Din, M.F.M., Methane emission by sectors: a comprehensive
717 review of emission sources and mitigation methods. *Renewable and Sustainable Energy Reviews*, 16(7), pp.5059-5070.
718 <https://doi.org/10.1016/j.rser.2012.04.008>, 2012.~~